International Journal of Systems Science

ISSN: 0020-7721 (Print) 1464-5319 (Online) Journal homepage: www.tandfonline.com/journals/tsys20

Necessary and sufficient condition for existence of two-degree-of-freedom feedback loop factorisation and comparison of zeros in compensator strategies

Marek Dlapa & Libor Pekar

To cite this article: Marek Dlapa & Libor Pekar (27 Feb 2026): Necessary and sufficient condition for existence of two-degree-of-freedom feedback loop factorisation and comparison of zeros in compensator strategies, International Journal of Systems Science, DOI: 10.1080/00207721.2026.2633322

To link to this article: https://doi.org/10.1080/00207721.2026.2633322

Published online: 27 Feb 2026.

INTERNATIONAL JOURNAL OF SYSTEMS SCIENCE
https://doi.org/10.1080/00207721.2026.2633322

Taylor & Francis
Taylor & Francis Group

Necessary and sufficient condition for existence of two-degree-of-freedom feedback loop factorisation and comparison of zeros in compensator strategies

Marek Dlapa and Libor Pekar

Faculty of Applied Informatics, Tomas Bata University in Zlin, Zlin, Czech Republic

ABSTRACT

Two cases of the two-degree-of-freedom (2DOF) feedback loop are compared after applying them to the third-order system with uncertain time delay, the fourth-order system with astatism and uncertain time delay and the oscillating system with astatism and uncertain time delay. All systems have periodic changes of some of their parameters. The necessary and sufficient condition for the existence of 2DOF factorisation is formed and proven. The uncertain time delay is treated using multiplicative uncertainty; the periodic changes of parameters are modelled using a general interconnection for the systems with parametric uncertainty in the numerator and denominator. The structured singular value denoted μ is used as a measure of robust performance and stability. For comparison, the D-K iteration and algebraic μ-synthesis are used for simple feedback loop controller derivation. The algebraic μ-synthesis is a new method for robust controller derivation comprising the structured singular value, algebraic control theory and metaheuristic algorithm solving multimodality of the cost function. Minimisation of the μ-function in the algebraic μ-synthesis is treated using the Differential Migration algorithm as a tool for global optimisation with subsequent tune-up using the Nelder–Mead simplex method. The final controllers are verified using the μ-plots and simulations for the worst-case perturbation and periodic changes of parameters with the maximum time delay.

ARTICLE HISTORY
Received 3 November 2025
Accepted 12 February 2026

KEYWORDS
Structured singular value; uncertain time delay; uncertain parameters; periodic changes; robust control; algebraic approach; factorisation; two-degree-of-freedom; necessary and sufficient condition; feedback loop; global optimisation; zero in compensator strategy

1. Introduction

The two-degree-of-freedom (2DOF) interconnection provides, in some cases, favourable properties with respect to treating the overshoot (Dlapa, 2021, 2025). In this paper, two modifications of 2DOF factorisation are discussed, giving slightly different outcomes with the controlled plants being the third-order system with uncertain time delay, the fourth-order system with astatism and uncertain time delay and the oscillating system with astatism and uncertain time delay. All controlled plants are the sets of plants with periodic changes in some of their parameters. The periodic changes of parameters are modelled in the scope of the linear fractional transformation (LFT) framework using parametric uncertainty system interconnection and robust stability and performance evaluation via the structured singular value denoted μ (SSV, Packard & Doyle, 1993). The necessary and sufficient condition for the existence of 2DOF factorisation is formed and proven, defining the possible cases of 2DOF interconnection application.

In the past decades, the parametric uncertainties have been a head issue of robust control. One of the first results was Mapping Theorem (Zadeh & Desoer, 1963) followed by Kharitonov Theorem (Barmish, 1984; Bialas, 1983; Kharitonov, 1978), Edge Theorem (Barmish, 1989; Bartlett et al., 1988; Sideris & de Gaston, 1986) and Generalised Kharitonov Theorem (Chapellat & Bhattacharyya, 1989), addressing conservatism in applications to a feedback loop with a SISO (single-input single-output) controller. One of the latest results is tree-structured decomposition (Barmish et al., 1990), yielding a general setup for the analysis of complicated closed-loop characteristic polynomials in the polynomial computation time and the results for specific multilinear structures (Barmish & Shi, 1990; Chapellat et al., 1993; Fu et al., 1995), considering the closed-loop character-

CONTACT Marek Dlapa dlapa@utb.cz Faculty of Applied Informatics, Tomas Bata University in Zlin, Nad Stranemi 4511, Zlin 760 05, Czech Republic
This article has been corrected with minor changes. These changes do not impact the academic content of the article.

istic polynomials corresponding to the series connections of interval plants.

This paper solves the problem of parametric uncertainties using the structured singular value and algebraic approache (Kučera, 1993; Vidyasagar, 1985) with subsequent optimisation using the metaheuristic algorithm (Dlapa, 2020, 2021), adding factorisation of a simple feedback controller to feed-forward, feedback and compensator part applicable to the two-degree-of-freedom feedback interconnection. This method solves both parametric and dynamic uncertainties, including uncertain time delay, and makes possible reference signal tracking without overshoot preserving the speed of response and robust performance. The Robust Control Design Toolbox for Time Delay Systems with Parametric and Periodic Uncertainties Using SSV (see Dlapa, 2019 with different definitions of parametric uncertainties, weights and their particular interconnections in the general parametric uncertainty interconnection) is applied to periodic uncertainties in the plant transfer function and uncertain time delay. The design of the controller is performed for both the two-degree-of-freedom and single feedback loop (2DOF and 1DOF see Dlapa, 2025) and two cases of 2DOF factorisation with modified general parametric uncertainty interconnection for the LFT framework (Dlapa, 2025).

The controller is derived by solving a Diophantine equation in the ring of Hurwitz-stable and proper rational functions ($\mathscr{S}$) for a nominal plant. The tuning parameters are optimised via a metaheuristic algorithm and a direct search method – Differential Migration (Dlapa, 2009, 2017) and Nelder–Mead simplex method, respectively, handling the problem of multimodality of the cost function. This method solves the problem of the impossibility of use of the performance weights with astatism and convergence to a global or even local minimum, leading to non-optimality of the resulting controller in the D-K iteration (Stein & Doyle, 1991).

The two strategies for zeros in the compensator of the two-degree-of-freedom structure (2DOF) are applied to both the D-K iteration (see Doyle, 1985) and algebraic μ-synthesis controller, demonstrating the differences between the standard and proposed method. The overall performance is verified by simulations of step response for the maximum values of time delay in the simple feedback loop and two-degree-of-freedom structure (1DOF and 2DOF).

The following notation is used: s denotes Laplace operator if not defined otherwise, $\|\cdot\|$ is H_∞ norm, $\overline{\sigma}(\cdot)$ is the maximum singular value, $\mathbb{N}$, $\mathbb{R}$, $\mathbb{R}^{n\times m}$, $\mathbb{C}$ and $\mathbb{C}^{n\times m}$ ($n, m \in \mathbb{N}$) are natural numbers, real numbers, real matrices, complex numbers and complex matrices, respectively, and $\mathbf{I}_n$ is the unit matrix of dimension n.

2. Preliminaries

Define $\mathbf{\Delta}$ as a set of block diagonal matrices

$$\begin{aligned}\mathbf{\Delta} \equiv \{&\mathrm{diag}[\delta_1^R\mathbf{I}_{r_1},\ldots,\delta_S^R\mathbf{I}_{r_S},\delta_1^C\mathbf{I}_{c_1},\ldots,\delta_T^C\mathbf{I}_{c_T},\\ &\Delta_1^R,\ldots,\Delta_F^R,\Delta_1^C,\ldots,\Delta_K^C]:\\ &\delta_s^R\in\mathbb{R}, s=1\ldots S, \delta_t^C\in\mathbb{C}, t=1\ldots T,\\ &\Delta_f^R\in\mathbb{R}^{m_f^1\times m_f^2}, f=1\ldots F,\\ &\Delta_k^C\in\mathbb{C}^{n_k^1\times n_k^2}, k=1\ldots K,\\ &r_1\ldots r_S, c_1\ldots c_T\in\mathbb{N},\\ &m_1^1\ldots m_F^1, m_1^2\ldots m_F^2, n_1^1\ldots n_K^1, n_1^2\ldots n_k^2\in\mathbb{N},\\ &s,t,f,k,S,T,F,K\in\mathbb{N}\}\end{aligned} \tag{1}$$

For consistency among all dimensions, the following condition must be held

$$\begin{aligned}\sum_{s=1}^{S} r_s+\sum_{t=1}^{T} c_t+\sum_{f=1}^{F} m_f^1+\sum_{k=1}^{K} n_k^1&=n\\ \sum_{s=1}^{S} r_s+\sum_{t=1}^{T} c_t+\sum_{f=1}^{F} m_f^2+\sum_{k=1}^{K} n_k^2&=m\end{aligned} \tag{2}$$

Definition 2.1: For $\mathbf{M}\in\mathbb{C}^{n\times m}$ is $\mu_{\mathbf{\Delta}}(\mathbf{M})$ defined as

$$\mu_{\mathbf{\Delta}}(\mathbf{M}) \equiv \frac{1}{\min\{\overline{\sigma}(\Delta):\Delta\in\mathbf{\Delta}, \det(\mathbf{I}-\mathbf{M}\Delta)=0\}} \tag{3}$$

If no such $\Delta\in\mathbf{\Delta}$ exists making $\mathbf{I}-\mathbf{M}\Delta$ singular, then $\mu_{\mathbf{\Delta}}(\mathbf{M})=0$.

3. Modelling of a general plant with parametric uncertainties and time delay via the LFT framework

Define a general family of plants described by the set of transfer functions with an uncertain numerator and denominator and uncertain time

delay:

$$\tilde{\mathbf{P}} \equiv \left\{ \begin{array}{c} \dfrac{b_n s^n + b_{n-1}s^{n-1} + \ldots + b_1 s + b_0}{a_n s^n + a_{n-1}s^{n-1} + \ldots + a_1 s + a_0} \, \mathrm{e}^{-\tau s} : \\ a_i \in [\bar{a}_i - da_i, \bar{a}_i + da_i], \\ b_i \in [\bar{b}_i - db_i, \bar{b}_i + db_i], \\ \tau \in [0, T_d], i = 0, 1, \ldots, n \end{array} \right\} \tag{4}$$

This set of plants corresponds to the interconnection in Figure 1, fitting into the linear fractional transformation (LFT) framework. For the perturbations $\delta_{a_i}, \delta_{b_i} \in \mathbb{R}$, $\delta_{del} \in \mathbb{C}$, the following conditions hold

$$|\delta_{a_i}| < 1, \quad |\delta_{b_i}| < 1, \quad |\delta_{del}| < 1, \; i = 0, 1, \ldots, n \tag{5}$$

The weights W_{a_i}, W_{b_i} and W_{del} must satisfy the following inequalities:

$$W_{a_i} = da_i/(\bar{a}_n s^{n-i}), \quad i = 0, 1, \ldots, n \tag{6}$$

$$W_{b_i} = db_i/(\bar{a}_n s^{n-i}), \quad i = 0, 1, \ldots, n \tag{7}$$

$$|W_{del}| > |1 - \mathrm{e}^{-T_d j\omega}|, \quad \text{for all } \omega \in \mathbb{R} \tag{8}$$

A set of plants (4) corresponding to the interconnection in Figure 1 can be transformed to the interconnections in Figure 2, where the sensitivity function, as a performance indicator, is included and $\tilde{\mathbf{P}}_{nom}$ with Δ_2 in feedback loop is the open-loop interconnection in Figure 1. The perturbation matrix Δ_2 is defined as follows:

$$\Delta_2 \equiv \begin{bmatrix} \Delta_a & 0 & 0 \\ 0 & \Delta_b & 0 \\ 0 & 0 & \delta_{del} \end{bmatrix} \tag{9}$$

$$\Delta_a \equiv \begin{bmatrix} \delta_{a_0} & 0 & \cdots & 0 \\ 0 & \delta_{a_1} & \cdots & 0 \\ \vdots & \vdots & \ddots & \vdots \\ 0 & 0 & \cdots & \delta_{a_n} \end{bmatrix} \tag{10}$$

$$\Delta_b \equiv \begin{bmatrix} \delta_{b_0} & 0 & \cdots & 0 \\ 0 & \delta_{b_1} & \cdots & 0 \\ \vdots & \vdots & \ddots & \vdots \\ 0 & 0 & \cdots & \delta_{b_n} \end{bmatrix} \tag{11}$$

For the stability and performance of the feedback loop depicted in Figure 2, Theorem 3.1 and subsequent Corollary 3.1 hold ($\mathbf{F}_L$ and $\mathbf{F}_U$ denote the lower and upper linear fractional transformation, respectively):

Theorem 3.1: *Assume* Δ_2 *defined by* (5), (9), (10), (11), *then the loop in Figure 2 is well-posed, internally stable and* $\|\mathbf{F}_L[\mathbf{F}_U(\mathbf{G}, \Delta_2), K]\|_\infty \leq 1$ *if and only if*

$$\sup_{\omega \in \mathbb{R}} \mu_{\tilde{\mathbf{\Delta}}}[\mathbf{F}_L(\mathbf{G}, K)(j\omega)] \leq 1 \tag{12}$$

with $\tilde{\mathbf{\Delta}} \equiv \left\{ \begin{bmatrix} \delta_1 & 0 \\ 0 & \Delta_2 \end{bmatrix} : |\delta_1| < 1, \delta_1 \in \mathbb{C} \right\}$, $\tilde{\mathbf{\Delta}} \subset \mathbf{\Delta}$.

The proof of Theorem 3.1 is in the appendix of this article.

The set of sensitivity functions $\tilde{\mathbf{S}}$ is defined as the set of transfer functions from the reference signal r to error e in Figure 3:

$$\tilde{\mathbf{S}} \equiv \left\{ \tfrac{1}{1+PK} : P \in \tilde{\mathbf{P}} \right\} \tag{13}$$

As the consequence of Theorem 3.1, the following sufficient condition for the robust stability and performance of the feedback loop in Figure 3 holds for the set of sensitivity functions $\tilde{\mathbf{S}}$ and a family of plants (4).

Corollary 3.1: *With assumptions* (6), (7), (8) *and for every* $P \in \tilde{\mathbf{P}}$ *defined by* (4) *and* (5), *the feedback loop in Figure 3 is well-posed, internally stable and* $\|SW_1\|_\infty \leq 1$ *for every* $S \in \tilde{\mathbf{S}}$ *if* (12) *holds.*

Proof: The proof follows as shown in Figure 1, inequalities (12), (5), definitions (6), (7), (8) and Theorem 3.1. ■

Note that equivalence in Theorem 3.1 does not hold in Corollary 3.1 because transport delay in the set $\tilde{\mathbf{P}}$ is treated by multiplicative uncertainty with some conservatism. If time delay in the set $\tilde{\mathbf{P}}$ and subsequent treating via multiplicative uncertainty are omitted, then the equivalence in Corollary 3.1 would hold.

4. Algebraic μ-synthesis

To the generalised feedback loop in Figure 4, the algebraic μ-synthesis can be applied where $\mathbf{G}$ denotes the generalised plant, $\mathbf{K}$ is the controller, Δ_{del} is the perturbation matrix, r is the reference and e is the output.

The multi-input multi-output (MIMO) system with l inputs and l outputs can be decoupled into l identical SISO plants. Then the nominal model can defined in terms of continuous-time transfer functions:

$$\mathbf{P}_{nom}(s) \equiv \begin{bmatrix} \mathbf{P}_{11}(s) & \cdots & \mathbf{P}_{1l}(s) \\ \vdots & \ddots & \vdots \\ \mathbf{P}_{l1}(s) & \cdots & \mathbf{P}_{ll}(s) \end{bmatrix} \tag{14}$$

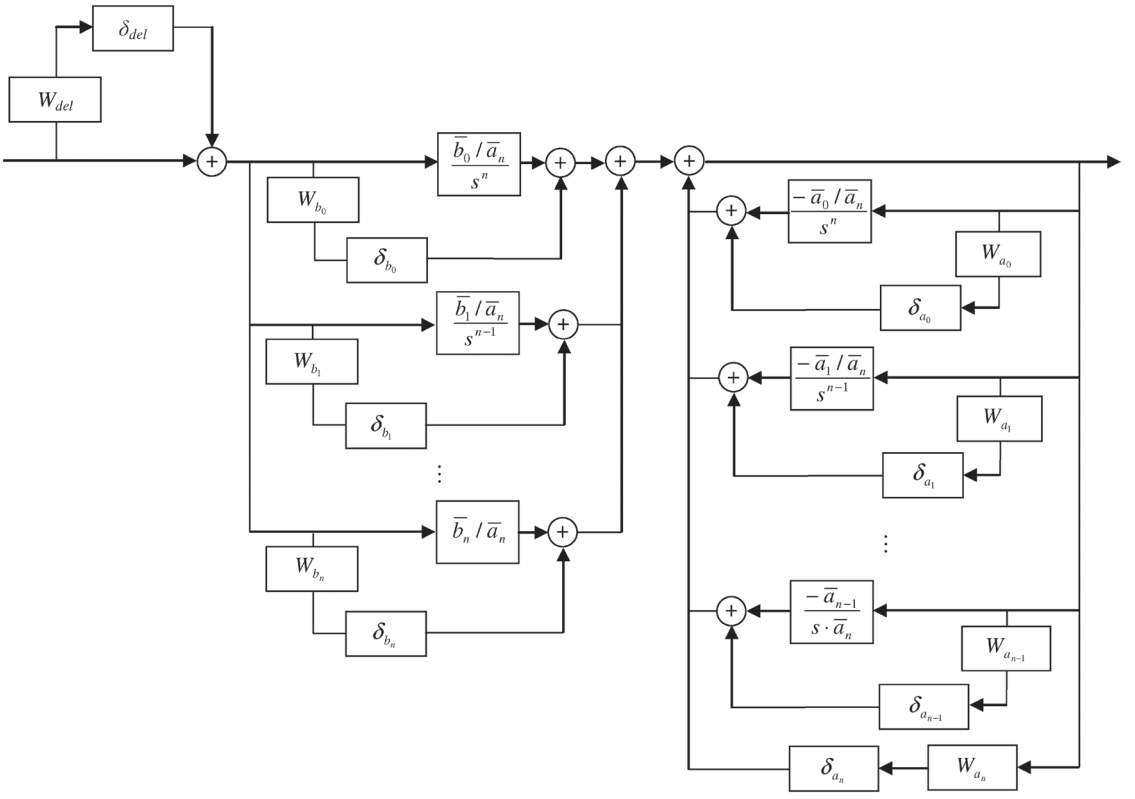

Figure 1. The general parametric uncertainty system interconnection for the LFT framework.

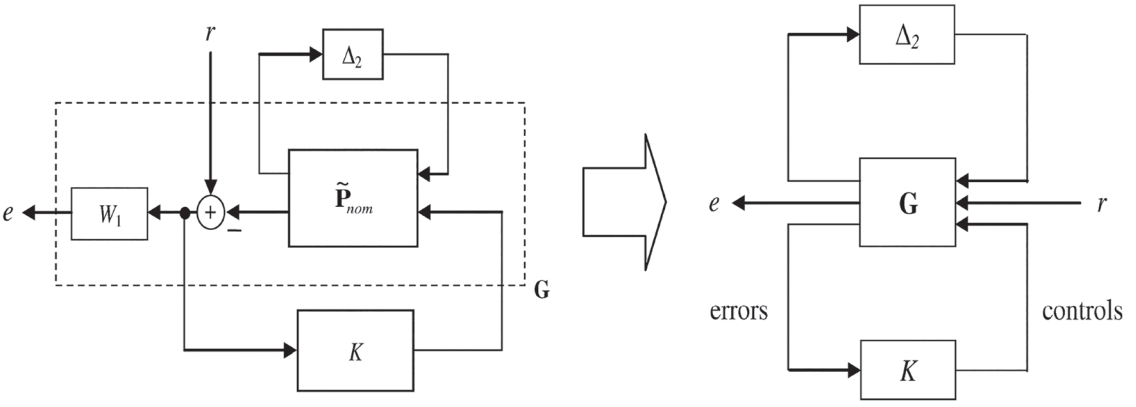

Figure 2. Closed-loop interconnection.

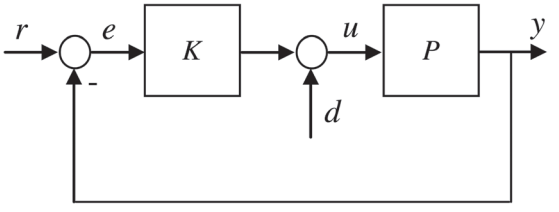

Figure 3. Feedback loop for $P \in \tilde{\mathbf{P}}$.

For decoupling the nominal plant $\mathbf{P}_{nom}(s)$ [$\mathbf{P}_{nom}(s)$ invertible], it is satisfactory to define the controller as

$$\mathbf{K}(s) = K(s)\mathbf{I}_l \frac{1}{P_{xy}(s)} adj[\mathbf{P}_{nom}(s)] \qquad (15)$$

where P_{xy} is an element of $adj[\mathbf{P}_{nom}(s)] = \det[\mathbf{P}_{nom}(s)] \cdot [\mathbf{P}_{nom}(s)]^{-1}$ with the highest degree of numerator {$adj[\mathbf{P}_{nom}(s)]$ denotes the adjugate matrix of $\mathbf{P}_{nom}$}. The definition of the decoupling matrix prevents the controller from cancelling any unstable poles or zeros so that the internal stability of the nominal feedback loop is held. The MIMO problem is reduced to finding a controller for the nominal feedback loop with the plant

$$\mathbf{P}_{dec}(s) = \frac{1}{P_{xy}(s)} \det[\mathbf{P}_{nom}(s)] \mathbf{P}_{nom}(s)^{-1} \mathbf{P}_{nom}(s)$$

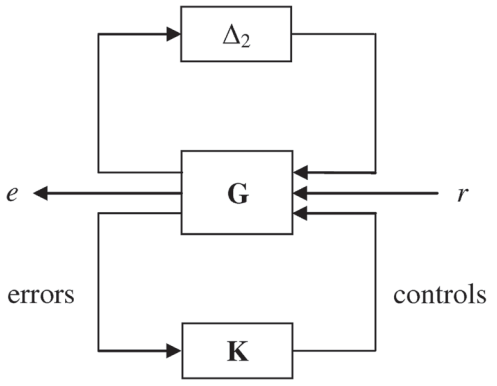

Figure 4. Closed-loop interconnection.

$$\mathbf{P}_{dec}(s) = \frac{1}{P_{xy}(s)}\det[\mathbf{P}_{nom}(s)]\mathbf{I}_l \tag{16}$$

From Equation (16) follows the nominal plant transfer function used in the algebraic μ-synthesis controller derivation:

$$P_{dec}(s) = \frac{1}{P_{xy}(s)}\det[\mathbf{P}_{nom}(s)] \tag{17}$$

Transfer function P_{dec} can be approximated by a system P^*_{dec} with a lower order than P_{dec}

$$P^*_{dec}(s) = \frac{b(s)}{a(s)} \tag{18}$$

and rewritten in terms of its coefficients and transformed to the elements of $\mathscr{S}$

$$P^*_{dec}(s) = \frac{\frac{b_n s^n + b_{n-1}s^{n-1} + \ldots + b_1 s + b_0}{(\alpha_1+s)(\alpha_2+s)\cdot\ldots\cdot(\alpha_n+s)}}{\frac{a_n s^n + a_{n-1}s^{n-1} + \ldots + a_1 s + a_0}{(\alpha_1+s)(\alpha_2+s)\cdot\ldots\cdot(\alpha_n+s)}} \tag{19}$$

The controller $K = N_K/(D_K F)$ is obtained by solving the Diophantine equation

$$AD_K F + BN_K = 1 \tag{20}$$

with $A, B, D_K, N_K, F \in \mathscr{S}$ and A, B coprime in $\mathscr{S}$. Equation (20) is the Bezout identity. All feedback controllers $N_K/(D_K F)$ are given by Youla parameterisation

$$K = \frac{N_K}{D_K F} = \frac{N_{K_0} - ATF}{D_{K_0}F + BTF}, N_{K_0}, D_{K_0} \in \mathscr{S} \tag{21}$$

where $N_{K_0}, D_{K_0} \in \mathscr{S}$ are particular solutions of (20), F is a predefined compensator and T is an arbitrary element of $\mathscr{S}$.

The controller K, satisfying Equation (20), guarantees the Hurwitz stability of the feedback loop in Figure 5. The Hurwitz stability is not a necessary condition for theorems related to robust stability and performance in the scope of the structured singular value theory but, without loss of generality, simplifies searching for the optimal or stabilising tuning parameters α_i with $i = 1, 2, \ldots n + n_1 + n_2$ and arbitrary transfer function $T \in \mathscr{S}$. If the controller or nominal plant has an astatism, then a stabilising controller exists even if performance weights with astatism are used, implying the non-existence of state-space solutions using DGKF formulae (see Doyle et al., 1989) due to zero eigenvalues of appropriate Hamiltonian matrices. Such a procedure results in zero steady-state error in the feedback loop with the controller obtained as a solution to Equation (20). This technique is possible in the scope of the standard μ-synthesis using neither DGKF formulae nor LMI approaches (see Gahinet & Apkarian, 1994), leading to numerical problems in most of real-world applications, though, according to standard control theory, the stabilising controller exists. This issue solves the algebraic μ-synthesis giving controllers satisfying robust stability and performance condition (12) even if the performance weight has an astatism in its transfer function.

The aim of the algebraic μ-synthesis is to find a controller satisfying the condition (12) rewritten in terms of tuning parameters α_i and t_i:

$$\sup_{\omega} \mu^u_{\mathbf{\Delta}}[\mathbf{F}_L(\mathbf{G}, \mathbf{K})(j\omega, \alpha_1, \ldots, \alpha_{n+n_1+n_2}, t_1, \ldots, t_{n_2})] \leq 1, \quad \omega \in [0, \infty) \tag{22}$$

ω is the angular velocity in Fourier transform, $n + n_1 + n_2$ is the order of the nominal feedback system, n_1 is the order of particular solution $K_0 = N_{K_0}/(D_{K_0}F)$, t_i are arbitrary parameters in $T = \frac{t_{n_2}s^{n_2} + t_{n_2-1}s^{n_2-1} + \ldots + t_1 s + t_0}{(\alpha_{n+n_1+1}+s)(\alpha_{n+n_1+2}+s)\cdot\ldots\cdot(\alpha_{n+n_1+n_2}+s)}$ and μ^u_{Δ} denotes the upper bound of the structured singular value of LFT on a generalised plant $\mathbf{G}$ and controller $\mathbf{K}$ corresponding to uncertainty set $\mathbf{\Delta}$ defined in (1).

Tuning parameters α_i are positive and constrained to the real axis since parameters of the controller transfer function have to be real and because non-real poles cause oscillations of the nominal feedback loop.

The cost function in (22) has many local extremes. So, local optimisation has a very low probability of finding a suitable or even stabilising solution. Here, this is overcome by optimisation using a metaheuristic algorithm with final tune-up by the Nelder–Mead simplex method solving the task more or less efficiently.

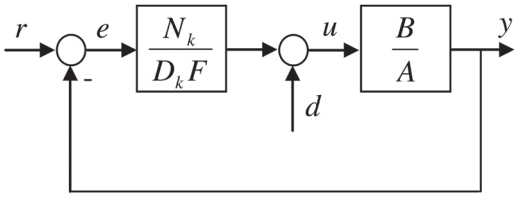

Figure 5. Nominal feedback loop.

Unlike the D-K iteration, the algebraic μ-synthesis does not include the approximation of scaling matrices in the upper bound μ calculation by transfer matrices, implying that there is no divergence from optimum and actual non-optimality of the final controller (Stein & Doyle, 1991) and uses the actual upper bound of μ-function for tuning the controller, instead, fixing this issue. The drawback is that the algebraic μ-synthesis uses an algorithm of global optimisation for the direct search of the nominal closed-loop poles as close to the optimum values as possible.

No other method is using an algebraic or Youla parameterisation approach for controller derivation using the structured singular value with robustness treated by structured uncertainty consequent upon Theorem 3.1. For this type of uncertainty, Theorem 3.1 and subsequent Corollary 3.1 can be used with any method for controller derivation using μ-function [e.g. D-K iteration and μ-K iteration (Lin et al., 1993)] as well as with the algebraic μ-synthesis.

5. Examples

5.1. Controlled sets of plants

The controlled plant families described by the set of transfer functions with uncertain time delay and uncertain coefficients in the numerator and denominator and the corresponding weights are defined as follows (t denotes time):

$$\tilde{\mathbf{P}}_1 \equiv \left\{ \begin{array}{c} \dfrac{b_{1,0}}{a_{1,3}s^3 + a_{1,2}s^2 + a_{1,1}s + a_{1,0}} \cdot \mathrm{e}^{-\tau_1 s} : \\ a_{1,0} = 1, \\ a_{1,1} \in [3 - 0.3, 3 + 0.3], \\ a_{1,1} = 3 + 0.3\sin(t), \\ a_{1,2} \in [3 - 0.3, 3 + 0.3], \\ a_{1,2} = 3 + 0.3\sin(t), \\ a_{1,3} = 1, \\ b_{1,0} \in [2 - 0.2, 2 + 0.2], \\ b_{1,1} = 2 + 0.2\sin(t), \\ \tau_1 \in [0, 4] \end{array} \right\} \tag{23}$$

$$W_{a_{1,1}} = 0.3/s^2 \tag{24}$$

$$W_{a_{1,2}} = 0.3/s \tag{25}$$

$$W_{b_{1,0}} = 0.2/s^3 \tag{26}$$

$$|W_{del1}| > |1 - \mathrm{e}^{4j\omega}|, \omega \in \mathbb{R} \Rightarrow W_{del1} = \frac{2s}{2s+1} \cdot 2.5 \tag{27}$$

$$W_{1,1}^{A} = \frac{1}{400s^2 + 40s} \tag{28}$$

$$W_{1,1}^{D-K} = \frac{1}{400s^2 + 40s + 0.00001} \tag{29}$$

$$\tilde{\mathbf{P}}_2 \equiv \left\{ \begin{array}{c} \dfrac{b_{2,0}}{a_{2,4}s^4 + a_{2,3}s^3 + a_{2,2}s^2 + a_{2,1}s} \cdot \mathrm{e}^{-\tau_2 s} : \\ a_{2,1} = 1, \\ a_{2,2} \in [3 - 0.3, 3 + 0.3], \\ a_{2,2} = 3 + 0.3\sin(0.1 \cdot t), \\ a_{2,3} \in [3 - 0.3, 3 + 0.3], \\ a_{2,3} = 3 + 0.3\sin(0.1 \cdot t), \\ a_{2,4} = 1, \\ b_{2,0} \in [2 - 0.2, 2 + 0.2], \\ b_{2,0} = 2 + 0.2\sin(0.1 \cdot t), \\ \tau_2 \in [0, 4] \end{array} \right\} \tag{30}$$

$$W_{a_{2,2}} = 0.3/s^2 \tag{31}$$

$$W_{a_{2,3}} = 0.3/s \tag{32}$$

$$W_{b_{2,0}} = 0.2/s^4 \tag{33}$$

$$|W_{del2}| > |1 - \mathrm{e}^{4j\omega}|, \omega \in \mathbb{R} \Rightarrow W_{del2} = \frac{2s}{2s+1} \cdot 2.5 \tag{34}$$

$$W_{2,1}^{A} = \frac{1}{400s^2 + 40s} \tag{35}$$

$$W_{2,1}^{D-K} = \frac{1}{400s^2 + 40s + 0.00001} \tag{36}$$

$$\tilde{\mathbf{P}}_3 \equiv \left\{ \begin{array}{c} \dfrac{b_{3,0}}{a_{3,3}s^3 + a_{3,1}s} \cdot \mathrm{e}^{-\tau_3 s} : \\ a_{3,1} \in [1 - 0.2, 1 + 0.2], \\ a_{3,1} = 1 + 0.2\sin(0.1 \cdot t), \\ a_{3,3} = 1, \\ b_{3,0} \in [1 - 0.2, 1 + 0.2], \\ b_{3,0} = 1 + 0.2\sin(0.1 \cdot t), \\ \tau_3 \in [0, 0.5] \end{array} \right\} \tag{37}$$

$$W_{a_{3,1}} = 0.2/s^2 \tag{38}$$

$$W_{b_{3,0}} = 0.2/s^3 \tag{39}$$

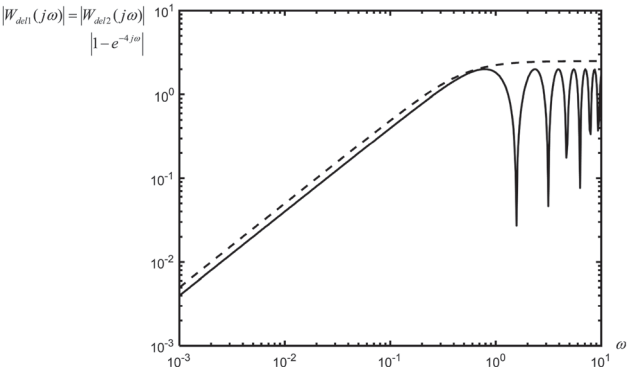

Figure 6. Bode plot of $|W_{del1}| = |W_{del2}|$ (dashed) and $|1 - e^{4j\omega}|$ (full).

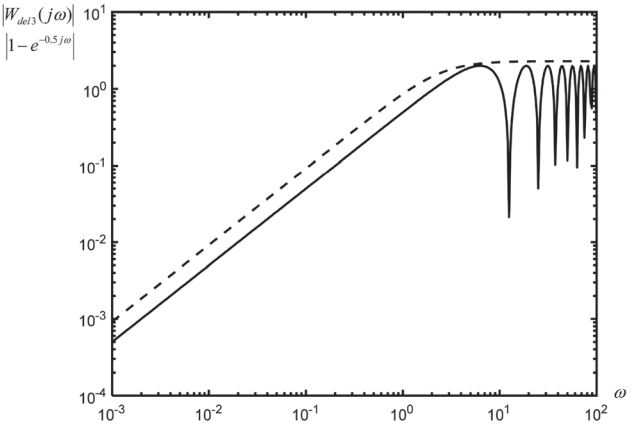

Figure 7. Bode plot of $|W_{del3}|$ (dashed) and $|1 - e^{0.5j\omega}|$ (full).

$$|W_{del3}| > |1 - e^{0.5j\omega}|, \omega \in \mathbb{R} \Rightarrow W_{del3} = \frac{2s}{2s+5} \cdot 2.3 \tag{40}$$

$$W_{3,1}^{A} = \frac{0.012}{400s^2 + 40s} \tag{41}$$

$$W_{3,1}^{D-K} = \frac{0.4}{400s^2 + 40s + 0.00001} \tag{42}$$

Weights W_{del1}, W_{del2} and W_{del3} correspond to the weight W_{del} in the set of plants $\tilde{\mathbf{P}}$ satisfying the condition (8) being the envelope curve of the right side of inequality (8) with small conservatism, as shown in the Bode plots of $|W_{del1}| = |W_{del2}|$, $|1 - e^{4j\omega}|$ and $|W_{del3}|$, $|1 - e^{0.5j\omega}|$ in Figures 6 and 7, respectively. Weights (24), (25), (26), (31), (32), (33), (38) and (39) follow from Equations (6) and (7) with respect to $\tilde{\mathbf{P}}_1$, $\tilde{\mathbf{P}}_2, \tilde{\mathbf{P}}_3 \subset \tilde{\mathbf{P}}$.

Predefined compensators of the algebraic μ-synthesis F_1, F_2 and F_3 corresponding with the sets $\tilde{\mathbf{P}}_1$, $\tilde{\mathbf{P}}_2$,

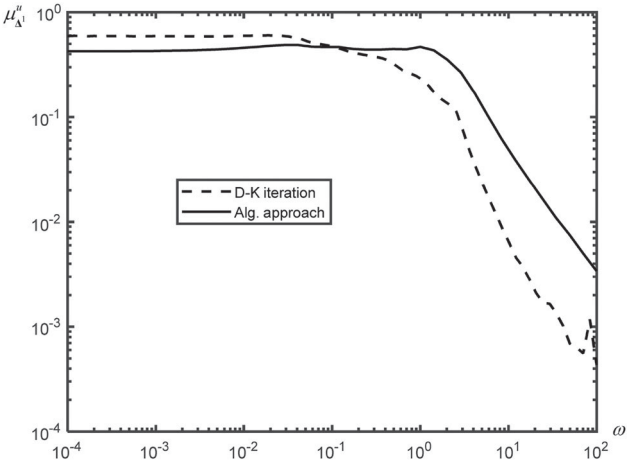

Figure 8. The upper bound μ-plot for the set of plants $\tilde{\mathbf{P}}_1$ with the controllers obtained by the D-K iteration and algebraic μ-synthesis.

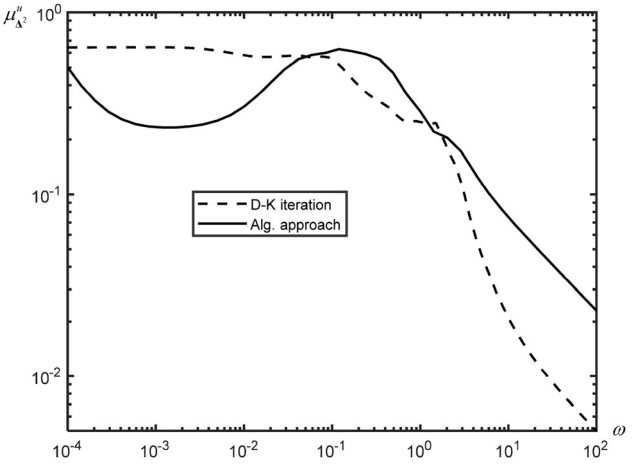

Figure 9. The upper bound μ-plot for the set of plants $\tilde{\mathbf{P}}_2$ with the controllers obtained by the D-K iteration and algebraic μ-synthesis.

$\tilde{\mathbf{P}}_3$ are defined so that asymptotic tracking is guaranteed:

$$F_1 = \frac{s}{\alpha_{1,4} + s} \tag{43}$$

$$F_2 = 1 \tag{44}$$

$$F_3 = 1 \tag{45}$$

5.2. Global optimisation using a metaheuristic algorithm

To overcome multimodality of the cost function (22), a metaheuristic algorithm Differential Migration is used (DM, Dlapa, 2009) due to shorter time needed for finding global minimum than other algorithms of this type

Table 1. DM parameters for the set of plants $\tilde{\mathbf{P}}_1$.

Parameter	Value
Arbitrary Polynomial	none
Min. Value of α	0
Max. Value of α	80
Number of Population	30
Jump Range	[0.2, 4]
Perturbation Constant	0.7
Max. Number of Migration Loops	90
Accepted Error	0
Cluster Distance	1.3

with final tune-up carried out by the Nelder–Mead simplex method. Parameters of DM for each controlled plant are in Tables 1– 3.

Final negated nominal feedback loop poles and arbitrary elements of $\mathscr{S}$ obtained via global optimisation and direct search method are as follows:

Set of plants $\tilde{\mathbf{P}}_1$:

$$\begin{aligned} &\alpha_{1,1} = 0.6207; \quad \alpha_{1,2} = 30.5718; \quad \alpha_{1,3} = 2.0358 \\ &\alpha_{1,4} = 0.0793; \quad \alpha_{1,5} = 1.3709; \quad \alpha_{1,6} = 1.5665 \\ &\text{Arbitrary element of } \mathscr{S}: \ T_1(s) = 0 \end{aligned} \tag{46}$$

Set of plants $\tilde{\mathbf{P}}_2$:

$$\begin{aligned} &\alpha_{2,1} = 0.0482; \alpha_{2,2} = 0.0591; \alpha_{2,3} = 0.5004 \\ &\alpha_{2,4} = 1.1622; \alpha_{2,5} = 1.3631; \alpha_{2,6} = 1.4148 \\ &\alpha_{2,7} = 1.7386 \\ &\text{Arbitrary element of } \mathscr{S}: T_2(s) = 0 \end{aligned} \tag{47}$$

Set of plants $\tilde{\mathbf{P}}_3$:

$$\begin{aligned} &\alpha_{3,1} = 1.28; \alpha_{3,2} = 1.32; \alpha_{3,3} = 1.18 \\ &\alpha_{3,4} = 1.16; \alpha_{3,5} = 1.30; \alpha_{3,6} = 0.10 \\ &\text{Arbitrary element of } \mathscr{S}: \ T_3(s) = \frac{8.8311s + 3.8037}{(1.30 + s)(0.10 + s)} \end{aligned} \tag{48}$$

Final controllers transfer functions corresponding to negated nominal feedback loop poles and arbitrary polynomial obtained from global optimisation (46)–(48) and controllers obtained via the D-K iteration using modified performance weights $W_{1,1}^{D-K}$, $W_{2,1}^{D-K}$ and $W_{3,1}^{D-K}$ are:

Set of plants $\tilde{\mathbf{P}}_1$:

$$K_1^A(s) = \frac{9.442s^3 + 19.1s^2 + 11.82s + 3.29}{s^3 + 33.24s^2 + 82.36s} \tag{49}$$

$$K_1^{D-K}(s) = \frac{(345s^3 + 488s^2 + 272s + 0.769) \cdot 10^{-4}}{s^3 + 0.974s^2 + 0.00292s + 1.02 \cdot 10^{-9}} \tag{50}$$

Set of plants $\tilde{\mathbf{P}}_2$:

$$K_2^A(s) = \frac{0.0700s^3 + 0.1805s^2 + 0.1178s + 0.0028}{s^3 + 3.286s^2 + 2.655s + 0.00079} \tag{51}$$

$$K_2^{D-K}(s) = \frac{\begin{array}{c}(-32.8s^4 + 281s^3 + 474s^2 \\ +118s + 0.856) \cdot 10^{-4}\end{array}}{\begin{array}{c}s^4 + 0.658s^3 + 2.52s^2 \\ +0.359s + 1.97 \cdot 10^{-7}\end{array}} \tag{52}$$

Set of plants $\tilde{\mathbf{P}}_3$:

$$K_3^A(s) = \frac{\begin{array}{c}4.22s^6 + 22.5s^5 + 28.6s^4 - 0.524s^3 \\ -11s^2 - 1.1s + 0.588\end{array}}{\begin{array}{c}s^6 + 10.1s^5 + 43.7s^4 + 99.3s^3 \\ +115s^2 + 59.4s + 8.58\end{array}} \tag{53}$$

$$K_3^{D-K}(s) = \frac{\begin{array}{c}(-3.305s^3 + 44.34s^2 \\ +10.56s + 0.103) \cdot 10^{-4}\end{array}}{\begin{array}{c}s^3 + 0.238s^2 + 0.0271s \\ -1.46 \cdot 10^{-8}\end{array}} \tag{54}$$

The upper bound μ plots in Figures 8–10 show that both controllers have the supremum of the upper bound μ below one and the robust stability and performance conditions in Corollary 3.1 are satisfied for all controlled plants with the maximum values of upper bound μ:

$$\begin{aligned} &\sup_{\omega} \mu_{\mathbf{\Delta}^1}^u[\mathbf{F}_L(\mathbf{G}_1, K_1^A)] = 0.488, \\ &\sup_{\omega} \mu_{\mathbf{\Delta}^1}^u[\mathbf{F}_L(\mathbf{G}_1, K_1^{D-K})] = 0.603, \\ &\sup_{\omega} \mu_{\mathbf{\Delta}^2}^u[\mathbf{F}_L(\mathbf{G}_2, K_2^A)] = 0.628, \\ &\sup_{\omega} \mu_{\mathbf{\Delta}^2}^u[\mathbf{F}_L(\mathbf{G}_2, K_2^{D-K})] = 0.644, \\ &\sup_{\omega} \mu_{\mathbf{\Delta}^3}^u[\mathbf{F}_L(\mathbf{G}_3, K_3^A)] = 0.654, \\ &\sup_{\omega} \mu_{\mathbf{\Delta}^3}^u[\mathbf{F}_L(\mathbf{G}_3, K_3^{D-K})] = 0.563 \end{aligned}$$

where $\omega \in [0, \infty)$, $\mathbf{\Delta}^1$, $\mathbf{\Delta}^2$, $\mathbf{\Delta}^3 \subset \tilde{\mathbf{\Delta}} \subset \mathbf{\Delta}$ and $\mathbf{G}_1$, $\mathbf{G}_2$, $\mathbf{G}_3$ correspond to the sets of plants $\tilde{\mathbf{P}}_1$, $\tilde{\mathbf{P}}_2$, $\tilde{\mathbf{P}}_3$, respectively, fitting into interconnections in Figures 1 and 2.

5.3. Factorisation for 2DOF feedback loop

The controllers for the 2DOF feedback loop [Figure 11(a,b) – algebraic μ-synthesis and D-K iteration,

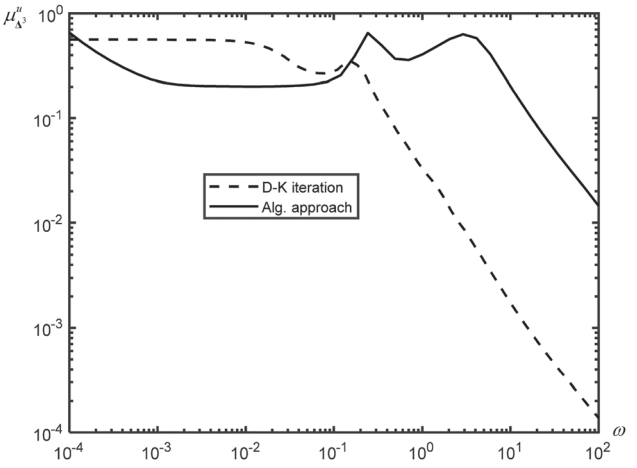

Figure 10. The upper bound μ-plot for the set of plants $\tilde{\mathbf{P}}_3$ with the controllers obtained by the D-K iteration and algebraic μ-synthesis.

Table 2. DM parameters for the set of plants $\tilde{\mathbf{P}}_2$.

Parameter	Value
Arbitrary Polynomial	none
Min. Value of α	0
Max. Value of α	2
Number of Population	30
Jump Range	[0.2, 4]
Perturbation Constant	0.7
Max. Number of Migration Loops	150
Accepted Error	0
Cluster Distance	1.25

Table 3. DM parameters for the set of plants $\tilde{\mathbf{P}}_3$.

Parameter	Value
Arbitrary Polynomial Degree	1
Min. Value of α	0
Max. Value of α	2
Min. Value of Arbitrary Parameters	0
Max. Value of Arbitrary Parameters	10
Number of Population	30
Jump Range	[0.2, 4]
Perturbation Constant	0.7
Max. Number of Migration Loops	100
Accepted Error	0
Cluster Distance	1.3

respectively] have the compensators ($n_{K_i^A 2M}$, $d_{K_i^A 2}$, $n_{K_i^{D-K} 2M}$, $d_{K_i^{D-K} 2}$) defined as fractions of the factors corresponding to the most stable zeros and all unstable poles of 1DOF controllers K_i^A and K_i^{D-K}. If there are complex conjugate zeros not aligned with the poles of the compensator, then the next most stable zero of K_i^A or K_i^{D-K} is moved to $n_{K_i^A 2M}$ or $n_{K_i^{D-K} 2M}$, and if there is no such zero, then the next least stable pole of K_i^A or K_i^{D-K} is moved to $d_{K_i^A 2}$ or $d_{K_i^{D-K} 2}$, so that

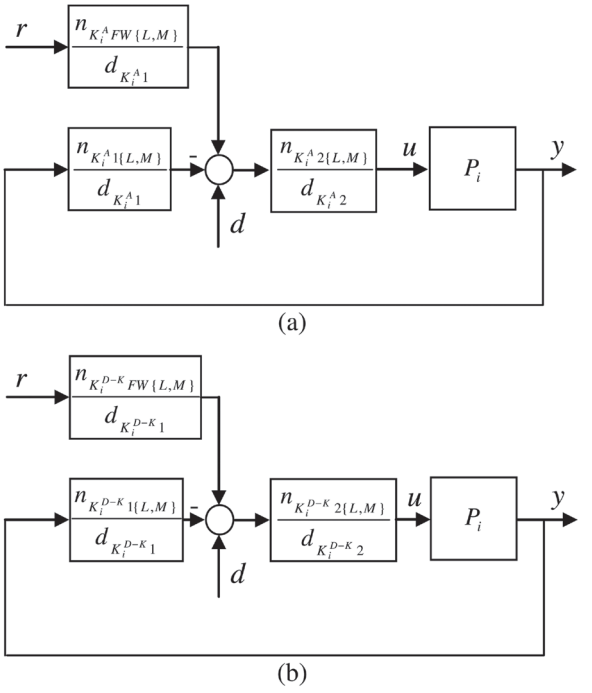

Figure 11. 2DOF feedback loop for $P_i \in \tilde{\mathbf{P}}_i$ and i $= 1, 2, 3$.

no single complex conjugate zero is in the numerator of the compensator and equivalently in the feedback part of the controller. If there is no unstable pole of K_i^A and K_i^{D-K}, then the most stable zero and least stable pole is used as the initial step. If K_i^A or K_i^{D-K} has non-strictly proper transfer function and degree of $d_{K_i^A 2}$ or $d_{K_i^{D-K} 2}$ is higher than the degree of K_i^A or K_i^{D-K} numerator then all zeros of K_i^A or K_i^{D-K} are moved to $n_{K_i^A 2M}$ or $n_{K_i^{D-K} 2M}$, respectively. Necessary condition for these steps is that no unstable pole of K_i^A and K_i^{D-K} is omitted from $d_{K_i^A 2}$ and $d_{K_i^{D-K} 2}$ so that the internal stability of the 2DOF feedback loop is preserved. The feedback ($n_{K_i^A 1M}$, $d_{K_i^A 1}$, $n_{K_i^{D-K} 1M}$, $d_{K_i^{D-K} 1}$) and feed-forward part ($n_{K_i^A FWM}$, $d_{K_i^A 1}$, $n_{K_i^{D-K} FWM}$, $d_{K_i^{D-K} 1}$) are defined by the factors corresponding to remaining zeros and poles of K_i^A and K_i^{D-K} with $n_{K_i^A FWM} = n_{K_i^A 1,0M}$ and $n_{K_i^{D-K} FWM} = n_{K_i^{D-K} 1,0M}$ ($n_{K_i^A 1,0M}$, $n_{K_i^{D-K} 1,0M}$ being the coefficients of $n_{K_i^A 1M}$ and $n_{K_i^{D-K} 1M}$ of zero exponent of s and $i = 1, 2, 3$).

In accordance with the procedure for the derivation of the 2DOF controller described in the previous paragraph, Theorem 5.1 follows with necessary and sufficient condition for the existence of 2DOF factorisation:

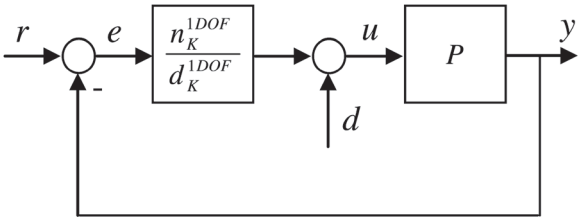

Figure 12. 1DOF feedback loop.

Theorem 5.1: *Define the 1DOF feedback loop as internally stable simple feedback loop in* Figure 12*, 1DOF controller as transfer function* $n_K^{1DOF}(s)/d_K^{1DOF}(s)$*, degree of* n_K^{1DOF} *as* ∂n_K^{1DOF} *and degree of* d_K^{1DOF} *as* ∂d_K^{1DOF}*. Assume that the minimum degree of compensator denominator* ($\partial d^c_{\min}$) *is equal to the number of unstable 1DOF feedback controller poles. If there are no unstable 1DOF controller poles, then* $\partial d^c_{\min} = 1$ *provided the 1DOF controller has at least one real pole, else* $\partial d^c_{\min} = 2$*. If the 1DOF controller has zero order, then* $\partial d^c_{\min} = 0$*.*

In the case of even $\partial d^c_{\min}$*, the 2DOF factorisation exists and the 2DOF feedback loop is internally stable if and only if* $\partial d^c_{\min} < \partial d_K^{1DOF}$*.*

In the case of odd $\partial d^c_{\min}$*,* $\partial d^c_{\min} < \partial n_K^{1DOF}$ *and numerator of the 1DOF controller does not have at least one real zero, the 2DOF factorisation exists and the 2DOF feedback loop is internally stable if and only if* $\partial d^c_{\min} + 1 < \partial d_K^{1DOF}$*.*

In the case of odd $\partial d^c_{\min}$*,* $\partial d^c_{\min} < \partial n_K^{1DOF}$ *and numerator of the 1DOF controller has at least one real zero or odd* $\partial d^c_{\min}$ *and* $\partial d^c_{\min} \geq \partial n_K^{1DOF}$*, the 2DOF factorisation exists and the 2DOF feedback loop is internally stable if and only if* $\partial d^c_{\min} < \partial d_K^{1DOF}$*.*

Proof: Sufficiency:

$\partial d^c_{\min}$ is equal to the minimum number of poles in the compensator for 2DOF feedback loop being internally stable provided all poles and zeroes are real or $\partial d^c_{\min} \geq \partial n_K^{1DOF}$. Further, mixed real and conjugate complex poles or zeroes cases will be discussed.

Even $\partial d^c_{\min}$: Complex conjugate zeros do not affect their inclusion in the compensator numerator.

Odd $\partial d^c_{\min}$, $\partial d^c_{\min} < \partial n_K^{1DOF}$ and numerator of the 1DOF controller does not have at least one real zero. The complex conjugate zeros cause the alignment of poles and zeros to even number of poles and zeros $\Rightarrow$ the number of the compensator poles must be increased by 1.

Odd $\partial d^c_{\min}$, $\partial d^c_{\min} < \partial n_K^{1DOF}$ and numerator of the 1DOF controller has at least one real zero or odd $\partial d^c_{\min}$ and $\partial d^c_{\min} \geq \partial n_K^{1DOF}$: Complex conjugate zeros do not affect their inclusion in the compensator numerator since there is at least one real zero making possible equality between poles and zeros moved into the compensator or all zeros of the 1DOF controller can be moved into the compensator.

Necessity:

All cases: If inequalities $\partial d^c_{\min} < \partial d_K^{1DOF}$ and $\partial d^c_{\min} + 1 < \partial d_K^{1DOF}$ in a particular case do not hold, then all poles and zeros would be in the compensator of 2DOF controller, hence, 2DOF and 1DOF would have the same interconnection. ■

Subscript M in numerators of 2DOF controllers stands for 'most stable' zeros in a compensator. In this paper, the least stable zeros (subscript L in numerators of 2DOF controllers) in the compensator are alternated with most stable ones and vice versa.

The necessary condition for the feedback part and compensator is ($i = 1, 2, 3$):

$$K_i^A = \frac{n_{K_i^A 1\{L,M\}} \cdot n_{K_i^A 2\{L,M\}}}{d_{K_i^A 1} \cdot d_{K_i^A 2}},;$$
$$K_i^{D-K} = \frac{n_{K_i^{D-K} 1\{L,M\}} \cdot n_{K_i^{D-K} 2\{L,M\}}}{d_{K_i^{D-K} 1} \cdot d_{K_i^{D-K} 2}} \tag{55}$$

Set of plants $\tilde{\mathbf{P}}_1$:

$$\begin{aligned}
\frac{n_{K_1^A 1L}}{d_{K_1^A 1}} &= \frac{9.442s^2 + 7.397s + 2.655}{s^2 + 33.24s + 82.36}, \\
\frac{n_{K_1^A FWL}}{d_{K_1^A 1}} &= \frac{2.655}{s^2 + 33.24s + 82.36}, \\
\frac{n_{K_1^A 2L}}{d_{K_1^A 2}} &= \frac{s + 1.239}{s} \\
\frac{n_{K_1^{D-K} 1L}}{d_{K_1^{D-K} 1}} &= \frac{0.0345s^2 + 0.0487s + 0.0271}{s^2 + 0.974s + 0.00292}, \\
\frac{n_{K_1^{D-K} FWL}}{d_{K_1^{D-K} 1}} &= \frac{0.0271}{s^2 + 0.974s + 0.00292}, \\
\frac{n_{K_1^{D-K} 2L}}{d_{K_1^{D-K} 2}} &= \frac{s + 0.00284}{s + 3.51 \cdot 10^{-7}}
\end{aligned} \tag{56, 57}$$

In this case, $n_{K_1^A 1M} = n_{K_1^A 1L}$, $n_{K_1^A FWM} = n_{K_1^A FWL}$, $n_{K_1^A 2M} = n_{K_1^A 2L}$, $n_{K_1^{D-K} 1M} = n_{K_1^{D-K} 1L}$, $n_{K_1^{D-K} FWM} = n_{K_1^{D-K} FWL}$, $n_{K_1^{D-K} 2M} = n_{K_1^{D-K} 2L}$.

Set of plants $\tilde{\mathbf{P}}_2$:

$$\begin{aligned}
\frac{n_{K_2^A 1L}}{d_{K_2^A 1}} &= \frac{0.06957s^2 + 0.1788s + 0.1134}{s^2 + 3.286s + 2.654},\\
\frac{n_{K_2^A FWL}}{d_{K_2^A 1}} &= \frac{0.1134}{s^2 + 3.286s + 2.654},\\
\frac{n_{K_2^A 2L}}{d_{K_2^A 2}} &= \frac{s + 0.0245}{s + 0.0002988}
\end{aligned} \tag{58}$$

$$\begin{aligned}
\frac{n_{K_2^{D-K} 1L}}{d_{K_2^{D-K}1}} &= \frac{\begin{array}{c}-32.75s^3 - 48.38s^2\\ -11.71s - 0.08523\end{array}}{s^3 + 0.6583s^2 + 2.522s + 0.3587}\\
&\quad \cdot 10^{-4},\\
\frac{n_{K_2^{D-K} FWL}}{d_{K_2^{D-K}1}} &= \frac{-8.523 \cdot 10^{-6}}{s^3 + 0.6583s^2 + 2.522s + 0.3587},\\
\frac{n_{K_2^{D-K} 2L}}{d_{K_2^{D-K}2}} &= \frac{s - 10.04}{s + 5.486 \cdot 10^{-7}}
\end{aligned} \tag{59}$$

$$\begin{aligned}
\frac{n_{K_2^A 1M}}{d_{K_2^A 1}} &= \frac{0.06957s^2 + 0.08082s + 0.001938}{s^2 + 3.286s + 2.654},\\
\frac{n_{K_2^A FWM}}{d_{K_2^A 1}} &= \frac{0.001938}{s^2 + 3.286s + 2.654},\\
\frac{n_{K_2^A 2M}}{d_{K_2^A 2}} &= \frac{s + 1.433}{s + 0.0002988}
\end{aligned} \tag{60}$$

$$\begin{aligned}
\frac{n_{K_2^{D-K} 1M}}{d_{K_2^{D-K}1}} &= \frac{\begin{array}{c}-32.75s^3 + 319.1s^2\\ +99.47s + 0.7287\end{array}}{s^3 + 0.6583s^2 + 2.522s + 0.3587}\\
&\quad \cdot 10^{-4},\\
\frac{n_{K_2^{D-K} FWM}}{d_{K_2^{D-K}1}} &= \frac{7.287 \cdot 10^{-5}}{s^3 + 0.6583s^2 + 2.522s + 0.3587},\\
\frac{n_{K_2^{D-K} 2M}}{d_{K_2^{D-K}2}} &= \frac{s + 1.175}{s + 5.487 \cdot 10^{-7}}
\end{aligned} \tag{61}$$

Set of plants $\tilde{\mathbf{P}}_3$:

$$\begin{aligned}
\frac{n_{K_3^A 1L}}{d_{K_3^A 1}} &= \frac{\begin{array}{c}4.22s^5 + 21.7s^4 + 24.3s^3\\ -5.25s^2 - 9.96s + 3.03\end{array}}{\begin{array}{c}s^5 + 9.87s^4 + 41.5s^3 + 89.94s^2\\ +94.86s + 38.02\end{array}},\\
\frac{n_{K_3^A FWL}}{d_{K_3^A 1}} &= \frac{3.03}{\begin{array}{c}s^5 + 9.87s^4 + 41.5s^3 + 89.94s^2\\ +94.86s + 38.02\end{array}},
\end{aligned}$$

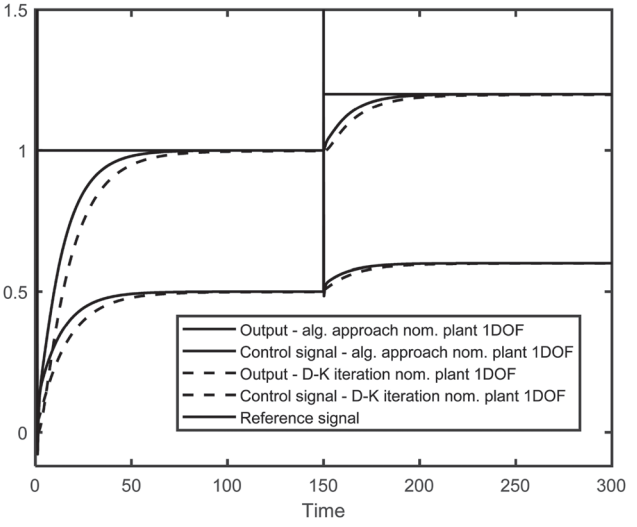

Figure 13. Simulation for the simple feedback loop and nominal plant of the set of plants $\tilde{\mathbf{P}}_1$.

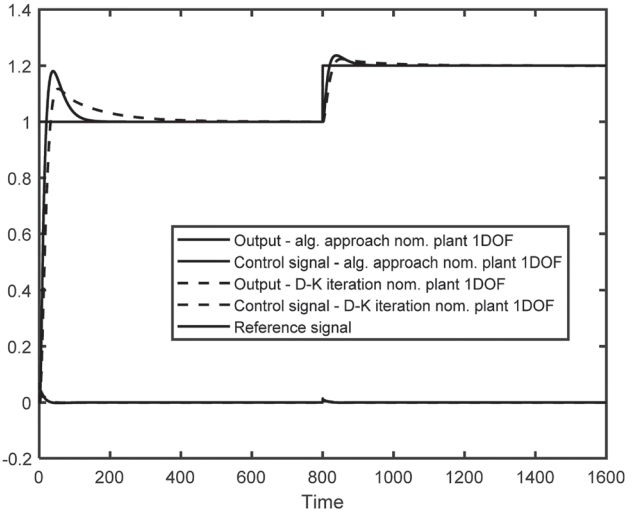

Figure 14. Simulation for the simple feedback loop and nominal plant of the set of plants $\tilde{\mathbf{P}}_2$.

$$\begin{aligned}
\frac{n_{K_3^A 2L}}{d_{K_3^A 2}} &= \frac{s + 0.194}{s + 0.226}
\end{aligned} \tag{62}$$

$$\begin{aligned}
\frac{n_{K_3^{D-K} 1L}}{d_{K_3^{D-K}1}} &= \frac{-33.1s^2 - 7.74s - 0.0753}{s^2 + 0.238s + 0.0271} \cdot 10^{-5},\\
\frac{n_{K_3^{D-K} FWL}}{d_{K_3^{D-K}1}} &= \frac{-7.53 \cdot 10^{-7}}{s^2 + 0.238s + 0.0271},\\
\frac{n_{K_3^{D-K} 2L}}{d_{K_3^{D-K}2}} &= \frac{s - 13.65}{s - 5.37 \cdot 10^{-7}}
\end{aligned} \tag{63}$$

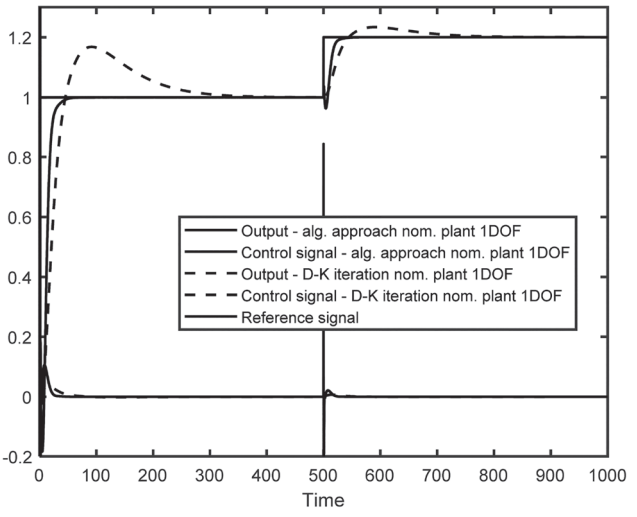

Figure 15. Simulation for the simple feedback loop and nominal plant of the set of plants $\tilde{\mathbf{P}}_3$.

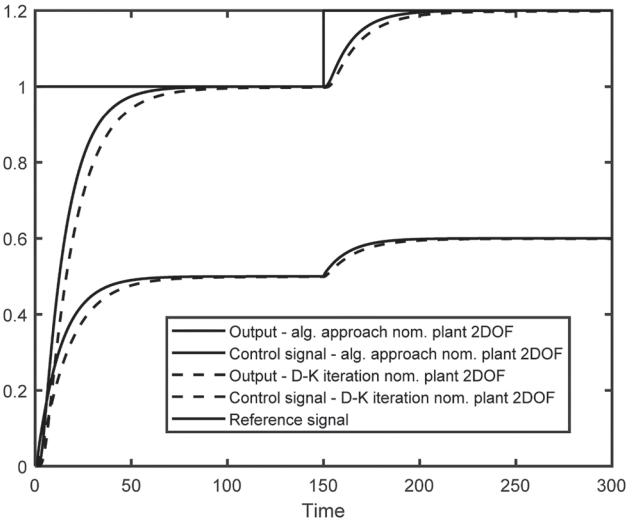

Figure 16. Simulation for the 2DOF feedback loop and nominal plant of the set of plants $\tilde{\mathbf{P}}_1$.

$$
\begin{aligned}
\frac{n_{K_3^A 1M}}{d_{K_3^A 1}} &= \frac{4.22s^5 + 8.11s^4 + 0.808s^3 - 3.29s^2 \\ +0.271s + 0.172}{s^5 + 9.87s^4 + 41.5s^3 + 89.94s^2 \\ +94.86s + 38.02}, \\
\frac{n_{K_3^A FWM}}{d_{K_3^A 1}} &= \frac{0.172}{s^5 + 9.87s^4 + 41.5s^3 + 89.94s^2 \\ +94.86s + 38.02}, \\
\frac{n_{K_3^A 2M}}{d_{K_3^A 2}} &= \frac{s + 3.42}{s + 0.226} \\
\frac{n_{K_3^{D-K} 1M}}{d_{K_3^{D-K} 1}} &= \frac{-33.1s^2 + 451s + 4.59}{s^2 + 0.238s + 0.0271} \cdot 10^{-5},
\end{aligned}
\tag{64}
$$

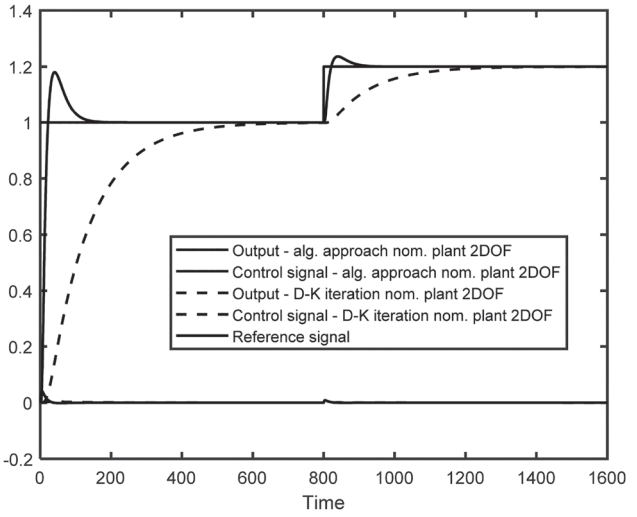

Figure 17. Simulation for te 2DOF feedback loop and nominal plant of the set of plants $\tilde{\mathbf{P}}_2$ – the least stable zeros in compensator.

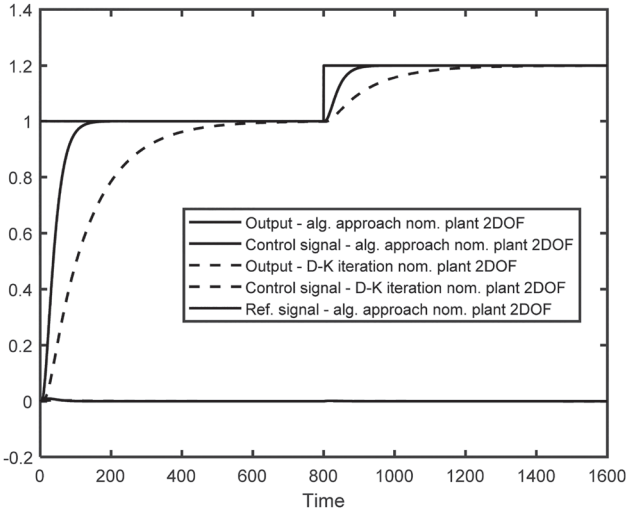

Figure 18. Simulation for the 2DOF feedback loop and nominal plant of the set of plants $\tilde{\mathbf{P}}_2$ – the most stable zeros in compensator.

$$
\begin{aligned}
\frac{n_{K_3^{D-K} FWM}}{d_{K_3^{D-K} 1}} &= \frac{4.59 \cdot 10^{-5}}{s^2 + 0.238s + 0.0271}, \\
\frac{n_{K_3^{D-K} 2M}}{d_{K_3^{D-K} 2}} &= \frac{s + 0.224}{s - 5.37 \cdot 10^{-7}}
\end{aligned}
\tag{65}
$$

5.4. Comparison study

All reference signals in the simulations are the reference signal r, all outputs are the output y and all control signals are control signal u in Figures 3 and 11 for each particular controller and set of plants.

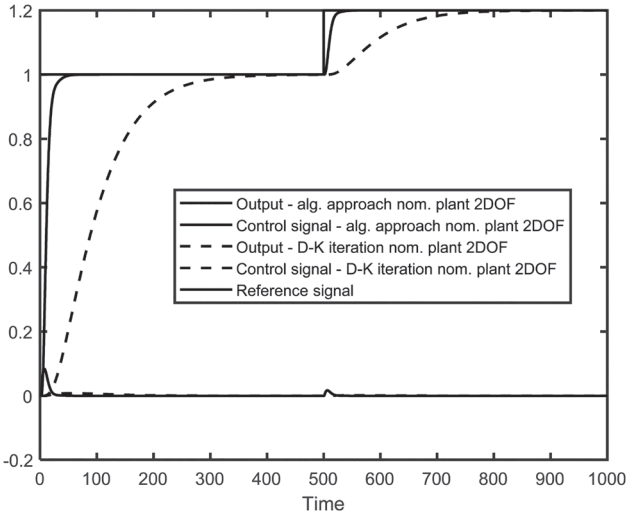

Figure 19. Simulation for the 2DOF feedback loop and nominal plant of the set of plants $\tilde{\mathbf{P}}_3$ – the least stable zeros in compensator.

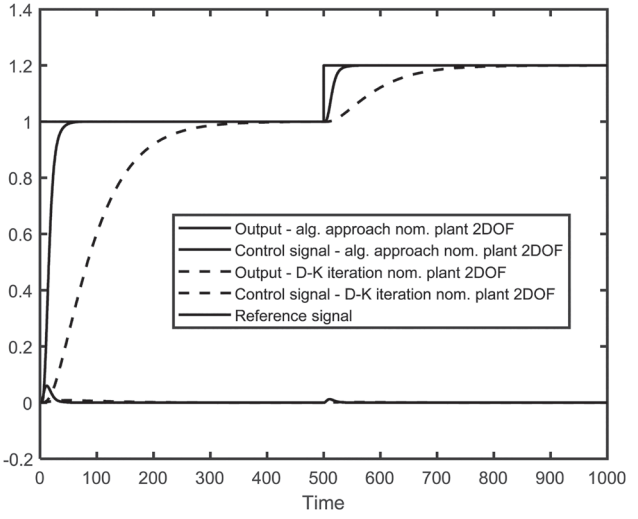

Figure 20. Simulation for the 2DOF feedback loop and nominal plant of the set of plants $\tilde{\mathbf{P}}_3$ – the most stable zeros in compensator.

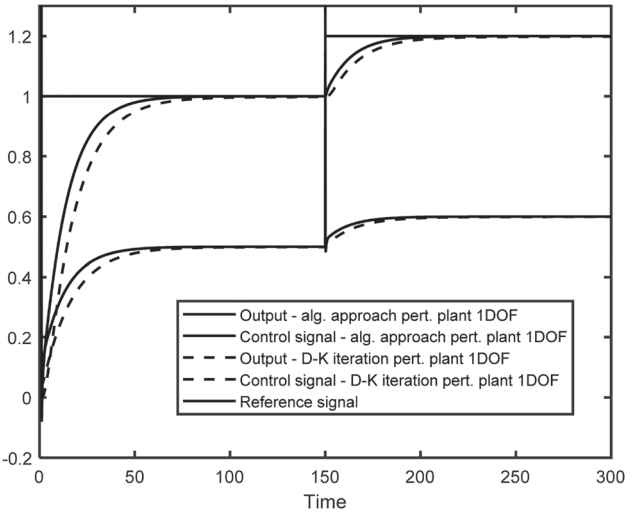

Figure 21. Simulation for the simple feedback loop and the worst-case perturbation – set of plants $\tilde{\mathbf{P}}_1$.

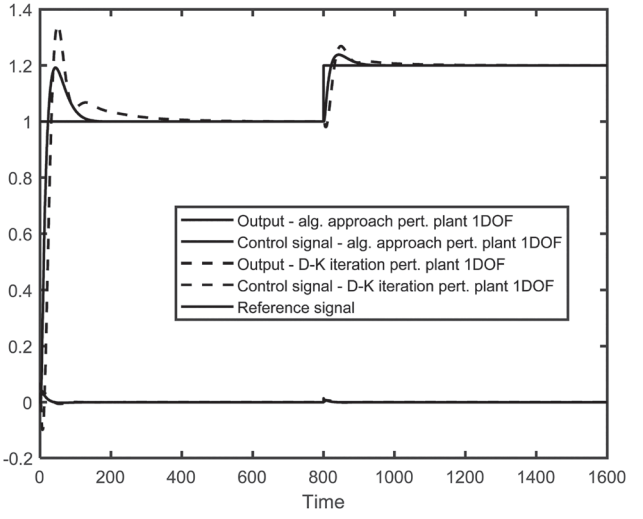

Figure 22. Simulation for the simple feedback loop and the worst-case perturbation – set of plants $\tilde{\mathbf{P}}_2$.

Simulations for nominal plants of the sets of plants $\tilde{\mathbf{P}}_1$, $\tilde{\mathbf{P}}_2$, $\tilde{\mathbf{P}}_3$ with respect to Figures 1 and 2 connected in simple feedback loop (Figure 3) and 2DOF feedback loop [Figure 11(a,b)] are in Figures 13–20. Simulations for sets of plants $\tilde{\mathbf{P}}_1$, $\tilde{\mathbf{P}}_2$, $\tilde{\mathbf{P}}_3$ perturbed by the worst-case perturbation (in the sense of the highest upper bound μ) in Figures 21–28 show that there is no significant deterioration compared to the nominal plants. For sets of plants $\tilde{\mathbf{P}}_2$ and $\tilde{\mathbf{P}}_3$ and simple feedback loop, there is an overshoot for the D-K iteration (see Figures 14 and 15) disappearing for 2DOF feedback loop for the least and most stable zeros in compensator of 2DOF controller (see Figures 17–20). The algebraic μ-synthesis has an overshoot for the set of plants $\tilde{\mathbf{P}}_2$ being resolved using the 2DOF feedback loop for most stable zeros in the compensator of 2DOF controller (Figure 18) but for least stable zeros of 2DOF controller, there is an overshoot (Figure 17).

Figures 13–28 show that the algebraic approach has faster set-point tracking than the D-K iteration controller and zero steady-state error for all sets of plants unlike the D-K iteration having non-zero steady state error for the set of plants $\tilde{\mathbf{P}}_1$ with no astatism in nominal plant for the simple feedback loop and 2DOF controller interconnection (Figures 13, 16, 21 and 24).

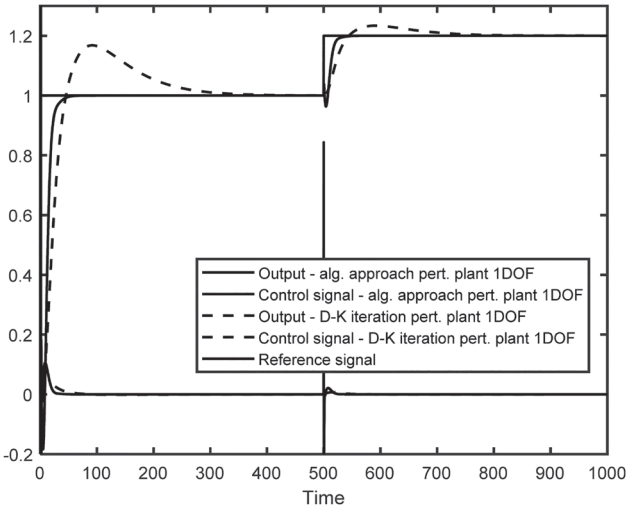

Figure 23. Simulation for the simple feedback loop and the worst-case perturbation – set of plants $\tilde{\mathbf{P}}_3$.

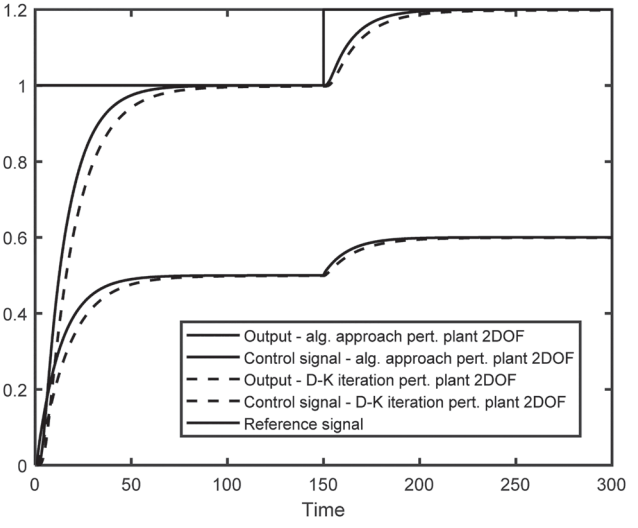

Figure 24. Simulation for the 2DOF feedback loop and the worst-case perturbation – set of plants $\tilde{\mathbf{P}}_1$.

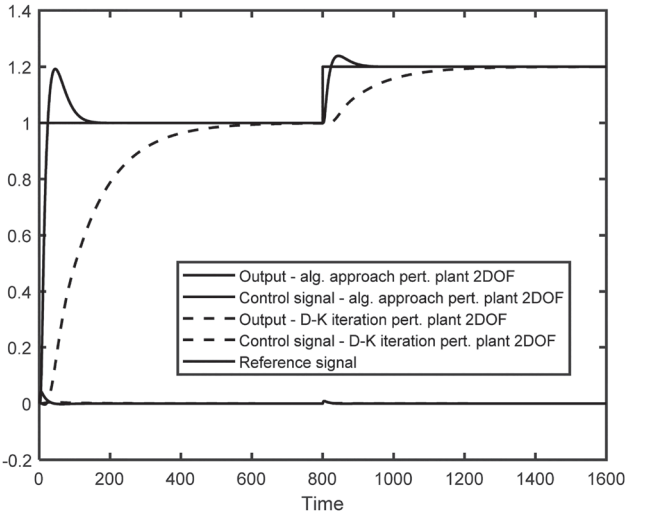

Figure 25. Simulation for the 2DOF feedback loop and the worst-case perturbation – set of plants $\tilde{\mathbf{P}}_2$ – the least stable zeros in compensator.

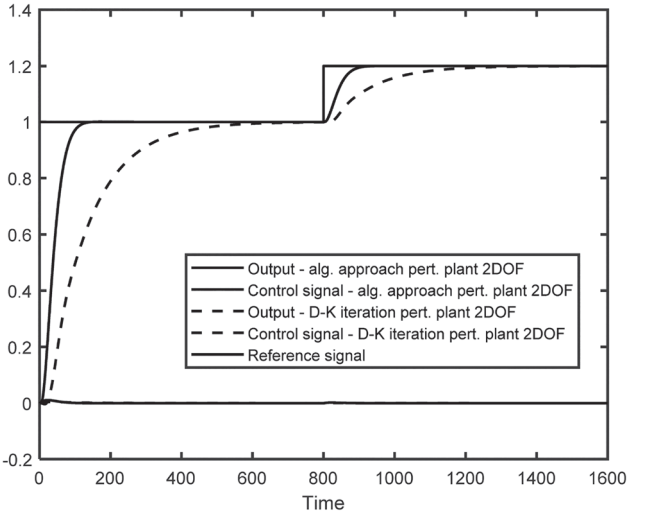

Figure 26. Simulation for the 2DOF feedback loop and the worst-case perturbation – set of plants $\tilde{\mathbf{P}}_2$ – the most stable zeros in compensator.

The reference signal tracking of the algebraic approach controller for the set of plants $\tilde{\mathbf{P}}_3$ is slightly faster if the least stable zeros are in compensator compared to the most stable ones, while the D-K iteration is not sensitive from this point of view, i.e. comparison of these two strategies (Figures 19, 20, 27 and 28).

Step responses for sets of plants $\tilde{\mathbf{P}}_1, \tilde{\mathbf{P}}_2, \tilde{\mathbf{P}}_3$ with periodic changes of their parameters demonstrate how the periodic changes of each parameter come out to the input (see Figures 29–31). Simulations for sets of plants $\tilde{\mathbf{P}}_1$, $\tilde{\mathbf{P}}_2$, $\tilde{\mathbf{P}}_3$ with periodic changes of their parameters in Figures 32–39 show that the stability is held for both simple feedback loop and 2DOF feedback loop (both strategies, i.e. the least and most stable zeros in the compensator of the 2DOF controller). Suppression of output oscillations is a bit higher for the algebraic approach compared to the D-K iteration for the set of plants $\tilde{\mathbf{P}}_3$ (Figures 34, 38 and 39), whereas for the sets of plants $\tilde{\mathbf{P}}_1$ and $\tilde{\mathbf{P}}_2$, there is no significant difference between the algebraic approach and D-K iteration from this point of view (Figures 32, 33 and 35–37).

Simulations with periodic changes of parameters were carried out with the maximum time delays consequent upon the plant definitions (23), (30), (37), i.e.

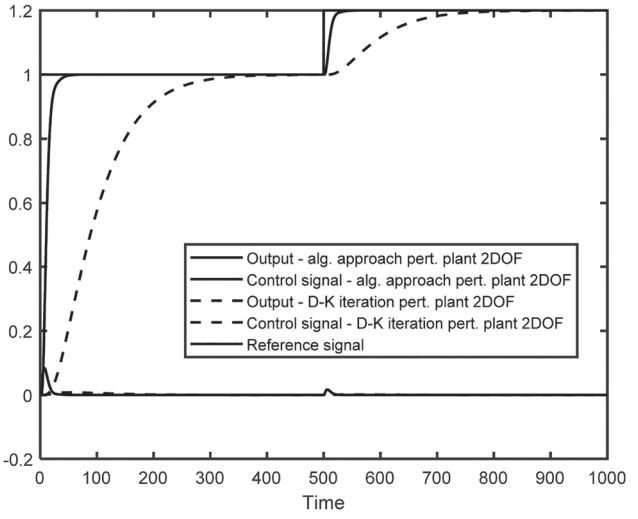

Figure 27. Simulation for the 2DOF feedback loop and the worst-case perturbation – set of plants $\tilde{\mathbf{P}}_3$ – the least stable zeros in compensator.

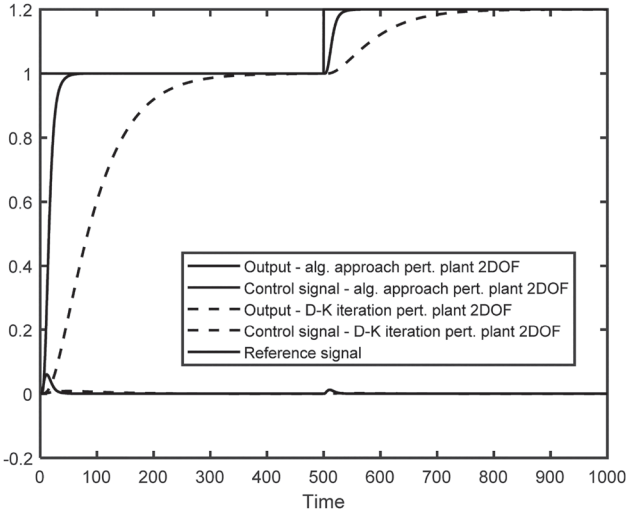

Figure 28. Simulation for the 2DOF feedback loop and the worst-case perturbation – set of plants $\tilde{\mathbf{P}}_3$ – most stable zeros in compensator.

$\tau_1 = \tau_2 = 4$ and $\tau_3 = 0.5$, and the fact that the maximum value of the μ-function does not increase its value if the time delay varies in the predefined intervals. So, the stability and performance do not deteriorate if the time delays are lower than their maximum values defined by their intervals.

6. Conclusion

The paper showed how the two strategies of 2DOF controller derivation, i.e. the least and most stable zeros in the compensator of 2DOF controller, affect

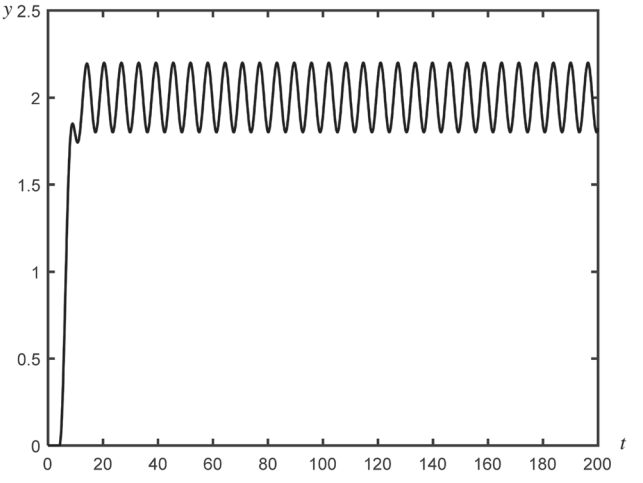

Figure 29. Step response for periodic changes of parameters and set of plants $\tilde{\mathbf{P}}_1$.

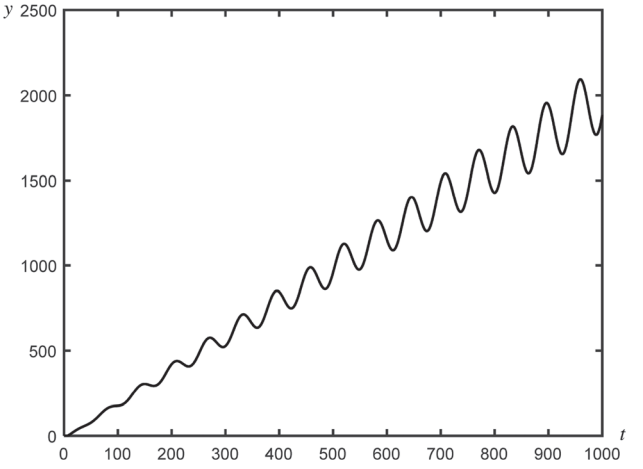

Figure 30. Step response for periodic changes of parameters and set of plants $\tilde{\mathbf{P}}_2$.

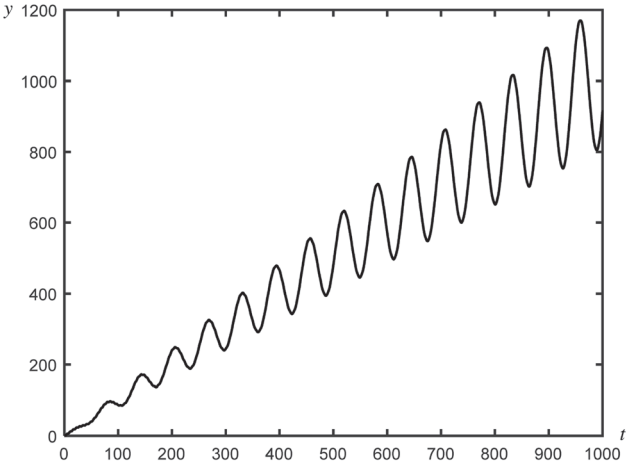

Figure 31. Step response for periodic changes of parameters and set of plants $\tilde{\mathbf{P}}_3$.

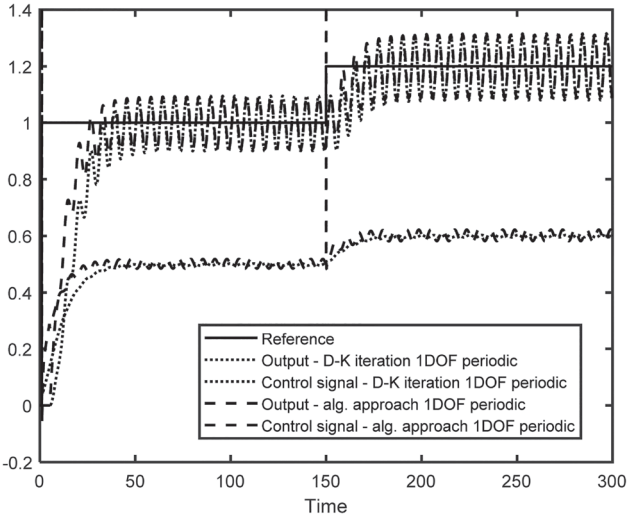

Figure 32. Simulations for the simple feedback loop with periodic changes – algebraic μ-synthesis, D-K iteration and set of plants $\tilde{\mathbf{P}}_1$.

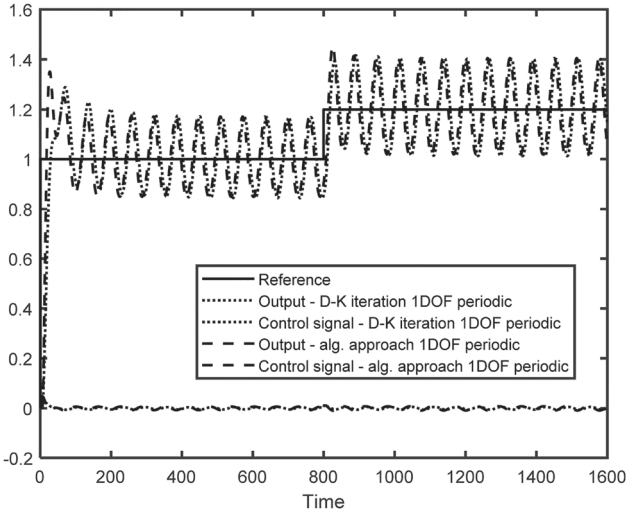

Figure 33. Simulations for the simple feedback loop with periodic changes – algebraic μ-synthesis, D-K iteration and set of plants $\tilde{\mathbf{P}}_2$.

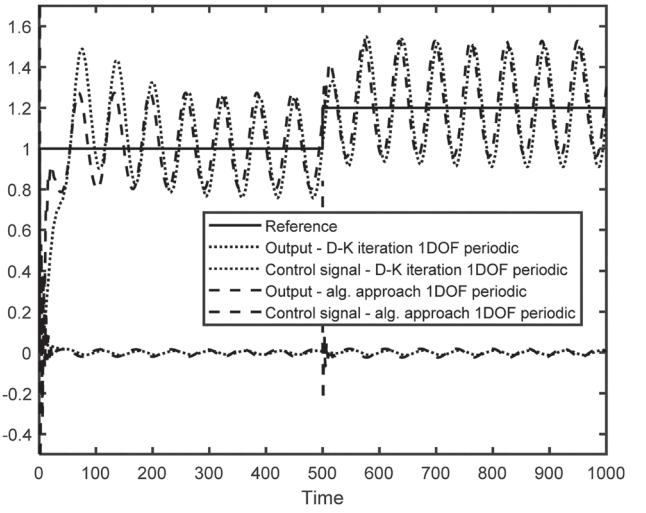

Figure 34. Simulations for the simple feedback loop with periodic changes – algebraic μ-synthesis, D-K iteration and set of plants $\tilde{\mathbf{P}}_3$.

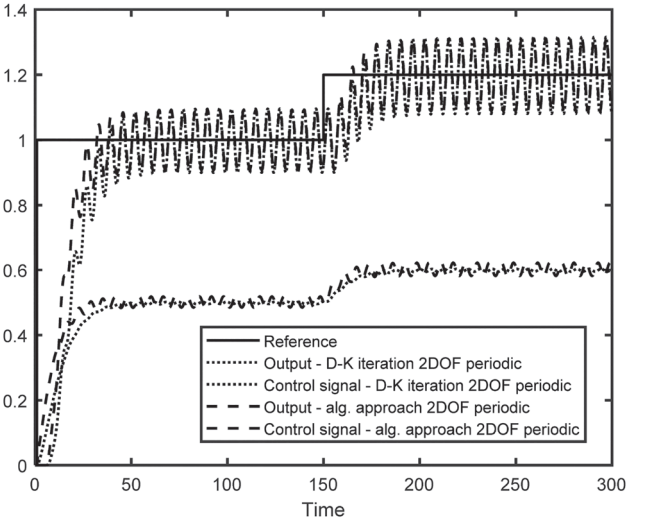

Figure 35. Simulations for the 2DOF feedback loop with periodic changes – algebraic μ-synthesis, D-K iteration and set of plants $\tilde{\mathbf{P}}_1$.

the controller behaviour in simulations with the sets of plants of the third- and fourth-order with and without astatism and oscillating set of plant with astatism, as well as the benefits of the algebraic μ-synthesis over the D-K iteration as the reference method, namely the controller structure can be chosen in advance and performance weight can be defined by transfer functions with astatism. The periodic changes of plant parameters were illustrated by step response simulations for each plant family. The feedback loop response simulation demonstrated that, though the D-K iteration acquired zero steady-state error for both controlled plants with astatism, an overshoot, as drawback, appeared in the time response of simple feedback loop, unlike the controller obtained using the algebraic approach having overshoot only for the 4th-order non-oscillating plant with astatism being resolved by the least stable zeros in the 2DOF feedback loop compensator strategy to monotonous time response to step-wise reference signal. For the oscillating plant with astatism and the least and most stable zeros in the compensator of 2DOF controller, small differences

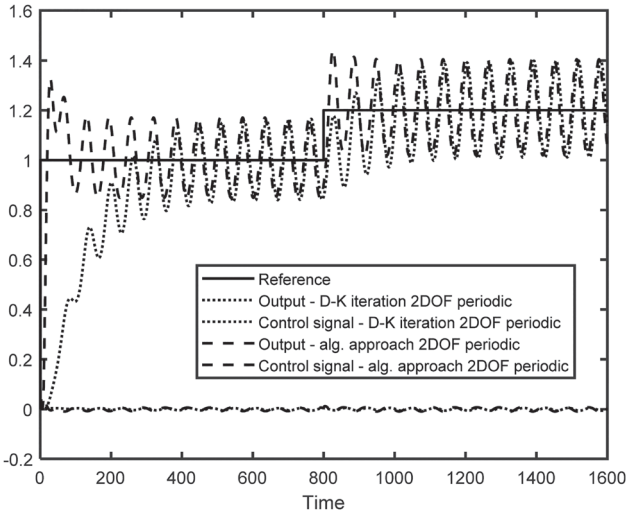

Figure 36. Simulations for the 2DOF feedback loop with periodic changes – algebraic μ-synthesis, D-K iteration and set of plants $\tilde{\mathbf{P}}_2$ – least stable zeros in compensator.

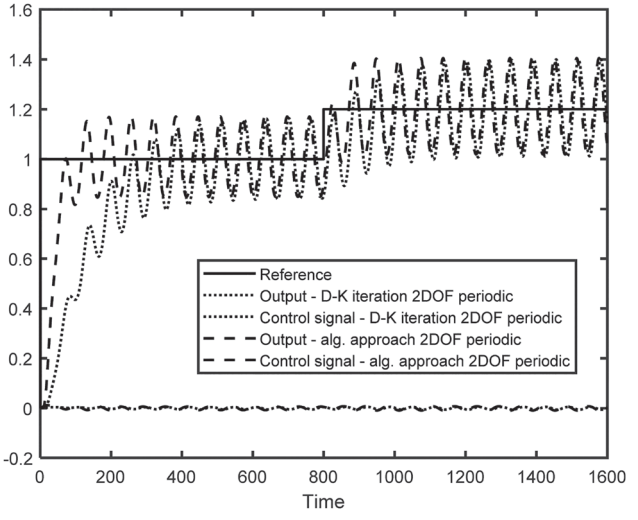

Figure 37. Simulations for the 2DOF feedback loop with periodic changes – algebraic μ-synthesis, D-K iteration and set of plants $\tilde{\mathbf{P}}_2$ – most stable zeros in compensator.

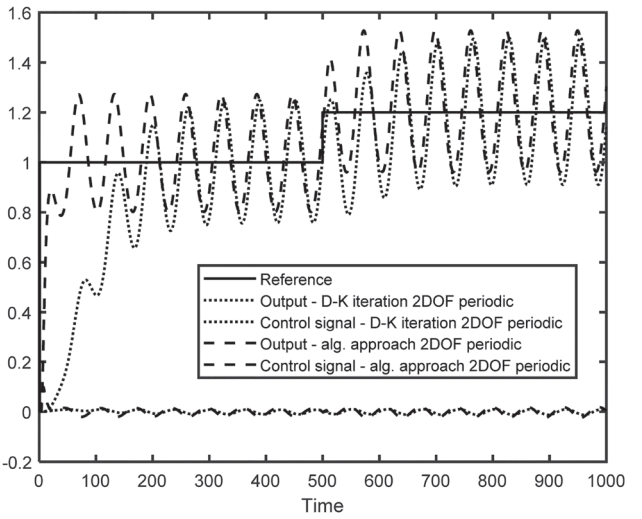

Figure 38. Simulations for the 2DOF feedback loop with periodic changes – algebraic μ-synthesis, D-K iteration and set of plants $\tilde{\mathbf{P}}_3$ – the least stable zeros in compensator.

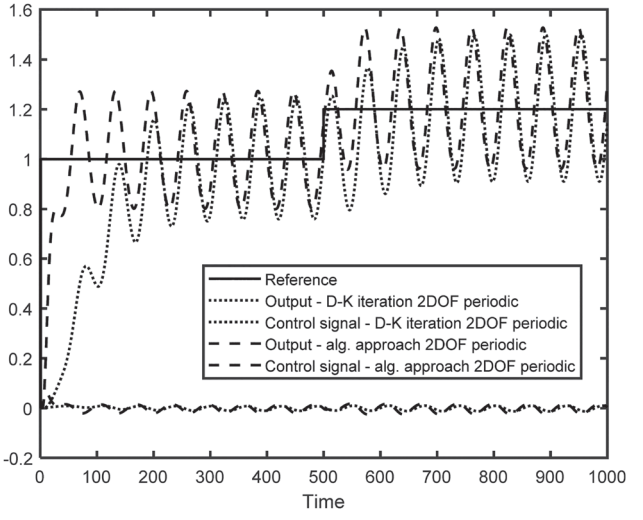

Figure 39. Simulations for the 2DOF feedback loop with periodic changes – algebraic μ-synthesis, D-K iteration and set of plants $\tilde{\mathbf{P}}_3$ – the most stable zeros in compensator.

appeared in the speed of set-point tracking of the algebraic μ-synthesis, unlike the D-K iteration without sensitivity to these two strategies of 2DOF controller derivation.

The factorisation procedure of the simple feedback loop to 2DOF interconnection for the algebraic μ-synthesis and the D-K iteration has been shown with the necessary and sufficient condition for the existence of 2DOF factorisation. The two strategies for 2DOF controller derivation were verified by the simulation of step response for three plant families comprising nominal, perturbed by the worst-case perturbation and periodic changes connected with the 2DOF controller.

The stability and performance is guaranteed for the whole range of time delays as a consequence of the structured singular value theory. So, only the maximum time delays are studied in simulations proving the functionality of both methods, i.e. the D-K iteration and algebraic μ-synthesis, following from the fact that the maximum upper bound of μ-function is lower than 1 with some margin, as shown in the μ-plots for each set of plant and the controller derivation method.

The only disadvantage of the algebraic μ-synthesis is the use of the global optimisation algorithm for the upper bound μ optimisation causing long time needed for obtaining a suitable controller and the fact that the optimality of the controller is not guaranteed. However, a similar issue is present in the D-K iteration causing non-optimality of the resulting D-K iteration controller consequent upon approximation of the scaling matrices D and D^{-1} by transfer function matrices $\hat{D}(s)$ and $\hat{D}^{-1}(s)$ making the upper bound of μ-function as close to the actual value of μ as possible.

Disclosure statement

No potential conflict of interest was reported by the author(s).

Funding

This work was supported by the European Regional Development Fund under the project CEBIA-Tech Instrumentation No. CZ.1.05/2.1.00/19.0376 and by the Ministry of Education, Youth and Sports of the Czech Republic within the National Sustainability Programme project No. LO1303 (MSMT-7778/2014).

Data availability statement

The Matlab simulation data that support the findings of this study are available from the corresponding author, Marek Dlapa, on the web https://dlapa.cz/homeeng.htm. All data is ethically correct and does not violate the protection of human subjects.

References

Barmish, B. R. (1984). Invariance of strict hurwitz property for polynomials with perturbed coefficients. *IEEE Transactions on Automatic Control*, *29*(10), 935–936. https://dx.doi.org/10.1109/TAC.1984.1103401

Barmish, B. R. (1989). A generalization of Kharitinov's four polynomial concept for robust stability with linearly dependent coefficient perturbations. *IEEE Transactions on Automatic Control*, *34*(2), 157–165. https://dx.doi.org/10.1109/9.21087

Barmish, B. R., Ackermann, J. E., & Hu, H. Z. (1990). The tree structured decomposition: A new approach to robust stability analysis. In *Conference on Information Sciences and Systems*.

Barmish, B. R., & Shi, Z. (1990). Robust stability of class of polynomials with coefficient depending multilinearly on perturbations. *IEEE Transactions on Automatic Control*, *35*(9), 1040–1043. https://dx.doi.org/10.1109/9.58532

Bartlett, A. C., Hollot, C., & Lin, H. (1988). Root locations of an entire polytope of polynomials: It suffices to check the edges. *Mathematics of Control, Signals and Systems*, *1*(1), 61–71. https://dx.doi.org/10.1007/BF02551236

Bialas, S. (1983). A necessary and sufficient conditions for stability of interval matrices. *International Journal of Control*, *37*(4), 717–722. https://dx.doi.org/10.1080/00207178308933004

Chapellat, H., & Bhattacharyya, S. P. (1989). An alternative proof of Kharitonov's theorem: Robust stability of interval plants. *IEEE Transactions on Automatic Control*, *34*(3), 306–311. https://dx.doi.org/10.1109/9.16420

Chapellat, H., Dahleh, M., & Bhattacharyya, S. P. (1993). Robust stability manifolds for multilinear interval systems. *IEEE Transactions on Automatic Control*, *38*(2), 314–318. https://dx.doi.org/10.1109/9.250482

Dlapa, M. (2009). Differential migration: Sensitivity analysis and comparison study. In *2009 IEEE Congress on Evolutionary Computation (IEEE CEC 2009)* (pp. 1729–1736). https://dx.doi.org/10.1109/CEC.2009.4983150.

Dlapa, M. (2017). Cluster restarted dm: New algorithm for global optimisation. In *Intelligent Systems Conference 2017 (IntelliSys 2017)* (pp. 1130–1135). https://dx.doi.org/10.1109/IntelliSys.2017.8324271.

Dlapa, M. (2019). Application of the robust control toolbox for time delay systems with parametric and periodic uncertainties using ssv to uncertain time delay system with astatism. In *The 5th IFAC Conference on Intelligent Control and Automation Science (ICONS 2019)* (pp. 134–139). https://dx.doi.org/10.1016/j.ifacol.2019.09.130.

Dlapa, M. (2020). Controller design for highly maneuverable aircraft technology using structured singular value and direct search method. In *The 2020 International Conference on Unmanned Aircraft Systems (ICUAS 2020)* (pp. 529–533). https://dx.doi.org/10.1109/ICUAS48674.2020.9214017.

Dlapa, M. (2021). Robust control design toolbox for general time delay systems via structured singular value: Unstable systems with factorization for two-degree-of-freedom controller. In *IEEE The 22nd International Conference on Industrial Technology (IEEE ICIT 2021)* (pp. 93–98). https://dx.doi.org/10.1109/ICIT46573.2021.9453505.

Dlapa, M. (2025). Structured singular value control with general two-degree-of-freedom feedback loop factorisation for single-input single-output systems. *IET the Journal of Engineering*, *2025*(1), e70115. https://dx.doi.org/10.1049/tje2.70115

Doyle, J. C. (1985). Structure uncertainty in control system design. In *24th IEEE Conference on decision and control* (pp. 260–265). https://dx.doi.org/10.1109/cdc.1985.268842.

Doyle, J. C., Glover, K., Khargonekar, P. P., & Francis, B. A. (1989). State-space solutions to standard H_2 and H_∞ control problems. *IEEE Transactions on Automatic Control*, *34*(8), 358–382. https://dx.doi.org/10.1109/9.29425

Doyle, J. C., Wall, J., & Stein, G. (1982). Performance and robustness analysis for structured uncertainty. In *21st IEEE Conference on Decision and Control* (pp. 629–636). https://doi.org/10.1109/cdc.1982.268218.

Fu, M., Dasgupta, S., & Blondel, V. (1995). Robust stability under a class of nonlinear parametric perturbations. *IEEE Transactions on Automatic Control*, *40*(2), 213–223. https://dx.doi.org/10.1109/9.341786

Gahinet, P., & Apkarian, P. (1994). A linear matrix inequality approach to H_∞ control. *International Journal of Robust and Nonlinear Control*, *4*(4), 421–449. https://dx.doi.org/10.1002/rnc.4590040403

Kharitonov, V. (1978). Asymptotic stability of an equilibrium position of a family of linear differential equations. *Differencialnye Uravneniya*, *14*, 2086–2088.

Kučera, V. (1993). Diophantine equations in control – a survey. *Automatica*, *29*(6), 1361–75. https://dx.doi.org/10.1016/0005-1098(93)90003-C

Lin, J. L., Postlethwaite, I., & Gu, D. W. (1993). μ-k iteration: A new algorithm for μ synthesis. *Automatica*, *29*(1), 219–224. https://dx.doi.org/10.1016/0005-1098(93)90185-V

Packard, A., & J. C. Doyle (1993). The complex structured singular value. *Automatica*, *29*(1), 71–109. https://dx.doi.org/10.1016/0005-1098(93)90175-S

Sideris, A., & de Gaston, R. (1986). Multivariable stability margin calculation with uncertainty correlated parameters. In *Conference on Decision and Control* (pp. 766–771). https://dx.doi.org/10.1109/cdc.1986.267458.

Stein, G., & Doyle, J. C. (1991). Beyond singular values and loopshapes. *AIAA Journal of Guidance and Control*, *29*(1), 5–16. https://dx.doi.org/10.2514/3.20598

Vidyasagar, M. (1985). *Control systems synthesis: A factorization approach*. MIT Press.

Zadeh, L., & Desoer, C. (1963). *Linear system theory: The state space approach*. McGraw-Hill.

Appendix. Proof of Theorem 3.1

Let $\beta > 0, \beta \in \mathbb{R}$. Define perturbations $\delta_{a_i}^\beta, \delta_{b_i}^\beta \in \mathbb{R}, \delta_{del}^\beta \in \mathbb{C}$

$$|\delta_{a_i}^\beta| < \frac{1}{\beta}, \quad |\delta_{b_i}^\beta| < \frac{1}{\beta}, \quad |\delta_{del}^\beta| < \frac{1}{\beta}, \quad i = 0, 1, \ldots, n \quad \text{(A1)}$$

Define perturbation matrix Δ_2^β:

$$\Delta_2^\beta \equiv \begin{bmatrix} \Delta_a^\beta & 0 & 0 \\ 0 & \Delta_b^\beta & 0 \\ 0 & 0 & \delta_{del}^\beta \end{bmatrix} \quad \text{(A2)}$$

$$\Delta_a^\beta \equiv \begin{bmatrix} \delta_{a_0}^\beta & 0 & \cdots & 0 \\ 0 & \delta_{a_1}^\beta & \cdots & 0 \\ \vdots & \vdots & \ddots & \vdots \\ 0 & 0 & \cdots & \delta_{a_n}^\beta \end{bmatrix} \quad \text{(A3)}$$

$$\Delta_b^\beta \equiv \begin{bmatrix} \delta_{b_0}^\beta & 0 & \cdots & 0 \\ 0 & \delta_{b_1}^\beta & \cdots & 0 \\ \vdots & \vdots & \ddots & \vdots \\ 0 & 0 & \cdots & \delta_{b_n}^\beta \end{bmatrix} \quad \text{(A4)}$$

Theorem A.1: *Assume* Δ_2^β *defined by* (A1), (A2), (A3), (A4), *then the loop in Figure 2 is well-posed, internally stable and* $\|\mathbf{F}_L[\mathbf{F}_U(\mathbf{G}, \Delta_2^\beta), K]\|_\infty \leq \beta$ *if and only if*

$$\sup_{\omega \in \mathbb{R}} \mu_{\tilde{\mathbf{\Delta}}^\beta}[\mathbf{F}_L(\mathbf{G}, K)(j\omega)] \leq \beta \quad \text{(A5)}$$

with

$$\tilde{\mathbf{\Delta}}^\beta \equiv \left\{ \begin{bmatrix} \delta_1^\beta & 0 \\ 0 & \Delta_2^\beta \end{bmatrix} : |\delta_1^\beta| < \tfrac{1}{\beta}, \delta_1^\beta \in \mathbb{C} \right\}, \quad \tilde{\mathbf{\Delta}}^\beta \subset \mathbf{\Delta}.$$

Proof: The proof with more general generalised plant $\mathbf{G}$ and perturbation set $\mathbf{\Delta}$ instead of $\tilde{\mathbf{\Delta}}^\beta$ is in Doyle et al. (1982) and Packard and Doyle (1993). ■

Proof of Theorem 3.1:

Proof: The proof follows from Theorem A.1 by defining $\beta = 1$. ■